Alma Mater Studiorum – Università di Bologna

DOTTORATO DI RICERCA IN

Bioingegneria

Ciclo XXVIII

Settore Concorsuale di afferenza: 09/G2 - BIOINGEGNERIA

Settore Scientifico disciplinare: ING - INF/06

Definition of neurophysiological indices to describe and quantify the cortical plasticity induced by neuro-rehabilitation

Presentata da: **Manuela Petti**

Coordinatore Dottorato

Prof.ssa Elisa Magosso

Relatore

Prof.ssa Laura Astolfi

Co-relatore

Prof.ssa Serenella Salinari

Contro-relatore

Prof.ssa Elisa Magosso

Esame finale anno 2016

Table of Contents

Introduction

The concept of neural plasticity refers to the brain ability to develop and adapt to changing environmental conditions or pathological conditions of different aetiology. In the latter case, brain functional reorganization is the phenomenon underlying the recovery (to different degrees) of impaired functions.

In clinical practice, the diagnosis of motor and cognitive impairment, as well as the understanding and assessment of the brain reorganization induced by neurorehabilitative interventions, are evaluated by behavioural scales that provide an indirect measure of brain plasticity through its behavioural manifestations, but not directly in the brain.

While the need of quantifiable neurophysiological measures of the processes occurring in the brain before, during and after the recovery of an impaired function is strongly felt in the field of neurorehabilitation, the methodological limitations in the extraction of relevant, stable and reliable information from brain signals (especially from those that can be easily collected from patients in a clinical environment) have so far prevented the inclusion of such procedure in the clinical practice.

The general objective of my PhD project was to develop a methodology for the definition and analysis of neurophysiological indices able to provide a stable and reliable measure of changes in the brain activity and organization, with the aim to:

i) support a diagnosis of motor and cognitive impairments on the basis of cortical modifications induced by neurorehabilitation;
ii) provide a neurophysiological description of the modifications in brain activity and organization subtending a functional recovery;

iii) allow the evaluation of the effects of (conventional and innovative) rehabilitation treatments in terms of brain reorganization (neurophysiological outcome measures of a treatment);

iv) describe specific properties in the brain general organization to be correlated with the outcome of the intervention, with possible prognostic/decision support value.

For this purpose, my research activity was focused on the development of an approach for the extraction of neurophysiological indices from non-invasive estimation of the cerebral activity and connectivity based on electroencephalographic (EEG) recordings. In fact, EEG provides an effective means to investigate both the temporal and the spectral activity of the brain, capturing the dynamics of brain processes (due to its excellent time resolution) and thus its organization and reorganization in time. Moreover, it is suitable for extensive usage in a clinical context and can be applied to patients in a wide range of clinical conditions.

Spectral and functional indices can be computed from EEG recorded during the execution of specific tasks (e.g. motor imagery, motor execution), but also from resting state brain activity, to capture both specific and general brain functional modifications. While results detected in the first case are directly linked to the impaired functions, the evaluation of changes detectable at rest can provide information about the basic structure of the brain organization that may be related to a pathology and significantly modified by a therapeutic intervention.

Brain activity and its changes in time are investigated here at three different interconnected levels that correspond to the three Sections of this thesis. For each of these, I evaluated the methods at the state of the art and proposed methodological advancements directly inspired by open problems presented by the nature of the data and by the clinical problem.

Experimental data used in this research activity were acquired during an extensive clinical study, involving a group of 56 unilateral stroke patients subjected to a twelve-sessions upper limb motor rehabilitative intervention based on Motor Imagery (MI). A subgroup of randomly selected patients were trained in the MI task with the support of Brain Computer Interface (BCI). All patients were also subjected to two neurophysiological screening sessions, prior and after training intervention.

The application of the developed methods to such data allowed to return a proof of the nature, quality and properties of the brain description and quantitative indices that can be derived from data easily recordable from a wide range of patients.

In Section I, brain functional modifications are investigated by means of EEG signals spectral analysis and statistical scalp maps. After a description of the state of the art, methodological developments are proposed with the aim to**:**

- quantify the entity of the desynchronization elicited in specific scalp regions;
- highlight the reinforcement of motor-related EEG patterns generated in the affected hemisphere of stroke patients undergoing a BCI-based training.

After the preliminary level of investigation performed with the study of changes in brain activity, in Section II brain connectivity estimation is proposed as a way to assess brain plasticity. Indeed, as the healing process is based on a reorganization of brain circuits, brain connectivity measures can be seen as the main tool for its investigation. Starting with the Granger causality concept and related state of the art multivariate time-domain connectivity estimator, i.e. Granger causality test, and its frequency domain equivalent estimator called Partial Directed Coherence (PDC) technique, the methodological contributions developed during this PhD project will be

described. Such advancements were mainly aimed to overcome the existing limitations in the evaluation of brain connectivity changes at the level of single-subject, needed to deal with the intrinsic variability characterizing patients.

In Section III, the graph theory approach is described and applied with the aim to capture brain networks properties modulated by an intervention, and thus underlying plasticity phenomena. The methodological developments reported here include new ad hoc descriptors of brain connectivity, introduced to evaluate specific properties related to the pathological condition under investigation and novel advanced approaches for the interpretation of brain connectivity patterns.

Finally, a general conclusion, reporting the main contributions achieved within this PhD project, their possible impact and their future development, closes this PhD thesis.

The study involving 56 post-stroke patients, including the MI and BCI-assisted MI training and the pre- and post- training EEG screening, was designed and performed by the team of the Neuroelectrical Imaging and BCI Lab (NEILab) at Fondazione Santa Lucia, IRCCS, Rome, Italy. All data reported in this thesis were collected in this laboratory.

The study related to motifs (subgraphs or "building blocks" of a network as a whole) was performed at the Computational Cognitive Neuroscience Laboratory of the Indiana University, Bloomington, USA, during a three-month abroad period performed during the PhD course.

The Appendix reports the complete list of papers published during the PhD course as a result of the research here described.

Section I

Evaluation of changes induced in brain activity by BCI-assisted MI training

1.1 Introduction

Mental practice in the form of movement imagination (Motor Imagery, MI) has long been envisaged as a cognitive strategy to enhance post-stroke motor recovery (Malouin and Richards 2010). Significant efforts have been made toward identifying the neural mechanisms underlying MI and their relationship with improved sensory-motor recovery (De Vico Fallani et al. 2013; Hanakawa, Dimyan, and Hallett 2008; Kaiser et al. 2012; Sharma,

Baron, and Rowe 2009). The rationale behind the application of MI to stroke rehabilitation is that mental practice with motor content engages areas of the brain that control movement execution (Cicinelli et al. 2006; Sharma and Baron 2013). Such reiterated engagement of motor areas is intended to influence brain plasticity phenomena, improving the recovery process (Cramer et al. 2011; Dimyan and Cohen 2011). Nevertheless, evidence for a clinical benefit of MI remains debatable. Although several studies have reported promising results (Gaggioli et al. 2006; Liu et al. 2009; Page, Levine, and Leonard 2007), a recent large, randomized, controlled study in subacute stroke patients reported no significant clinical improvement of MI practice as add-on therapy to standard treatment or compared with mental practice without motor content (Ietswaart et al. 2011). One possible reason for this lack of effect could be attributed to an unclear definition of the content of such mental practice (i.e., the impossibility to verify the actual brain activity related to the MI task).

In this context, EEG-based Brain-computer interfaces (BCIs) operated by MI can provide a valuable approach to support mental motor practice by allowing direct monitoring of the patient's adherence to such task-specific training.

As known, BCIs allow one to control external devices through direct brain activity recognition by a computer—ie, bypassing neuromuscular-based systems (voice, use of a mouse or keyboard) (Wolpaw et al. 2002; Shih, Krusienski, and Wolpaw 2012), but BCI techniques have also developed to support motor and cognitive rehabilitation. For example a widely adopted BCI paradigm uses the modulation of electroencephalographic (EEG) activity that is induced by the imagination of movement. MI elicits event-related desynchronization (ie, a reduction in spectral power) that occurs within certain EEG frequency oscillations and primarily over the scalp in sensorimotor cortical regions contralateral to the

imagined part of the body (sensorimotor rhythms, mu rhythm) (Pfurtscheller and Lopes da Silva 1999). New scientific questions and requirements arose as a consequence of these new BCI uses to face the twofold need to improve:

- the understanding of the effects of a neurofeedback-based training on brain cortical activity;
- the efficacy of the intervention by a strategy defined on ad hoc basis for such a purpose.

With respect to BCI for communication and control, whose aim is to maximize the accuracy and the reliability of the recognition of the user's intention, EEG-based BCI application for rehabilitation purposes is specifically aimed to increase the neuroelectrical responsiveness of specific regions of the brain, to enforce the recovery of impaired functions. For these reasons, EEG-based BCI operated by MI can be a valuable approach to support mental motor practice to enhance post stroke arm motor recovery. As stroke lesions may result in a functional reduction of activity of the ipsilesional hemisphere associated with a correspondent increase in the contralesional one, rehabilitation strategies should aim at increasing the excitability of the affected hemisphere and/or decreasing that in the unaffected (Dimyan and Cohen 2011). The adherence to the task is aided by an appropriate features selection, aimed to increase motor-related neuroelectrical responsiveness of the affected hemisphere. However, such features are necessarily limited to a restricted number of channels, while the correct desynchronization pattern is not monitored during training. While monitoring the cortical activity of the subject during the training is important for the aforementioned purposes, the effects of the online classifications of trials into as either successful or failed relies on arbitrary choices of parameters and gains instead of on intrinsic properties of the activity recorded during the training.

In this section, a description of the experimental subjects and protocol used in all the applications described in this thesis is provided. Then statistical procedures for the evaluation of changes induced in task-related brain activity were applied to stroke patients EEG data. Furthermore, some methodological developments are here proposed with the aim to define new indexes able to**:**

- highlight the reinforcement of motor-related EEG patterns generated from the lesioned hemisphere of stroke patients provided by a specifically developed BCI-based training device (F. Pichiorri et al. 2011);
- describe the properties of neuroelectrical activations across BCI training sessions more appropriately than the usually adopted hit rate (behavioral performance).

1.2 Experimental Subjects

Fifty-six stroke patients (mean age, 60.38 ± 13.36 years; time since event, 3.6 ± 4.2 months) were enrolled from the rehabilitation hospital ward at Fondazione Santa Lucia, Rome, Italy. Inclusion criteria were: adults (older than 18 years); first-ever monolateral stroke causing any degree of motor deficit in the upper limb; ability to understand the task; and stability of clinical conditions. The exclusion criteria were presence of any medical condition other than stroke affecting motor ability in the upper limb and anything preventing proper EEG recording. All patients gave informed consent. The study was approved by the local ethical committee of Fondazione Santa Lucia and was performed according to the declaration of Helsinki.

All the patients were subjected to a screening session (PRE) during which a clinical assessment was performed and EEG signals were collected during 2 minutes of eyes-closed resting state and during the execution of

different motor tasks (as described below). For the clinical assessment, an expert physician, blinded regarding the study, evaluated all patients in terms of severity of clinical impairment (European Stroke Scale, ESS), upper limb function (Fugl-Meyer Assessment, upper limb section), residual muscle strength in the upper limb (Medical Research Council [MRC] scale) and spasticity in the upper limb (Modified Ashworth Scale, MAS).

Thirty-five of the 56 subjects accepted to participate to a rehabilitative intervention based on motor imagery in add-on to standard treatment (tau). The study design foresaw two intervention groups: an experimental group that received 1 month of BCI-supported MI training (*BCI group*, 20 patients) with 3 weekly sessions and a control patient group that received equally intensive MI training with no BCI assistance (Control [*CTRL*] *group*, 15 patients). The same research team responsible for the evaluation PRE training performed a post-training clinical and neurophysiological assessment (POST).

During the EEG data acquisition (PRE and POST sessions), the patient was comfortably seated in an armchair in a dimly lit room with their upper limbs resting on a desk. A computer screen was positioned on the desk in front of the patient to provide visual cues. EEG was acquired from 61 standard positions (according to the extended 10–20 International System) band pass–filtered between 0.1 and 70 Hz, digitized at 200 Hz, and amplified by a commercial EEG system. At the beginning of the session, EEG signals were recorded during 2 minutes of eyes-closed resting state. Each session was divided into runs, with 30 trials for each run. Each trial was temporally determined by a cursor appearing in the low center of the screen and moving toward the top at a constant velocity on a straight trajectory. During rest trials, the patient was asked to watch the cursors trajectory. During motor task trials, a green rectangle (occupying the last 4 seconds of cursor trajectory) appeared at the top of the screen. The patient was asked to start

performing the cued motor task when the cursor reached the green rectangle and to continue until the end of the trajectory (Figure 1.1). The command sequence was randomized (15 rest and 15 motor trials per run).

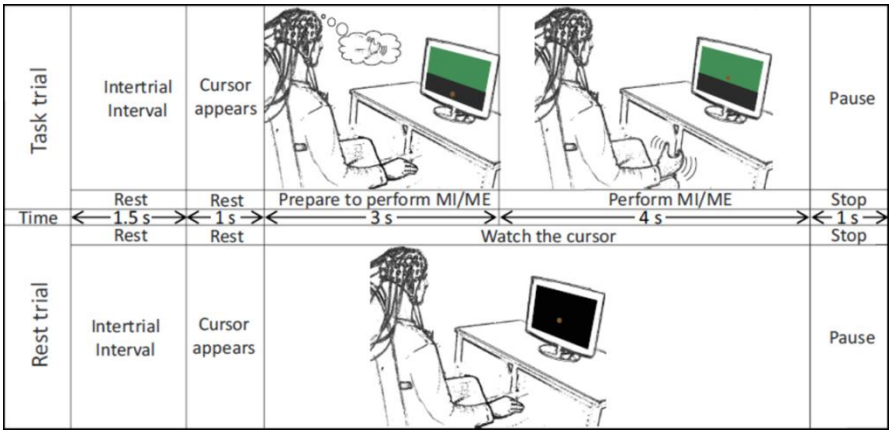

Figure 1.1. Timeline of rest and task trial during the screening session.

Each run was dedicated to a specific motor task that involved the unaffected or affected hand. Task A consisted of imaging a sustained grasping movement, whereas Task B entailed sustained complete extension of the finger. Tasks A and B were then trained during both MI interventions (BCI and CTRL). Patients were asked to either execute or imagine the simple movements (Tasks A and B) with the affected and unaffected hand in separate runs. The run sequence was randomized across patients. Depending on the severity of the motor deficit in the affected upper limb, patients were asked to execute the full movement or to just attempt it; in severely affected (plegic) patients, motor execution (ME) with the affected hand was not performed.

For the BCI group, EEG signals were collected also during the 12 training sessions from 31 positions over the sensory-motor areas. During these sessions, the patient was asked to control the movements of a virtual representation of his own stroke-affected hand throughout the imagination of

the described simple hand movements (visual neurofeedback). Each training session included 4 up to 8 runs (20 trials per run). Trials consisted of a baseline period (4 sec) followed by MI (max 10 sec) (Figure 1.2).

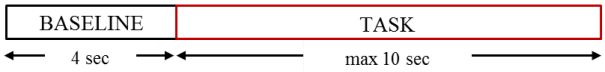

Figure 1.2. Timeline of task trial during the training sessions.

In figure 1.3 the rehabilitative protocol is shown.

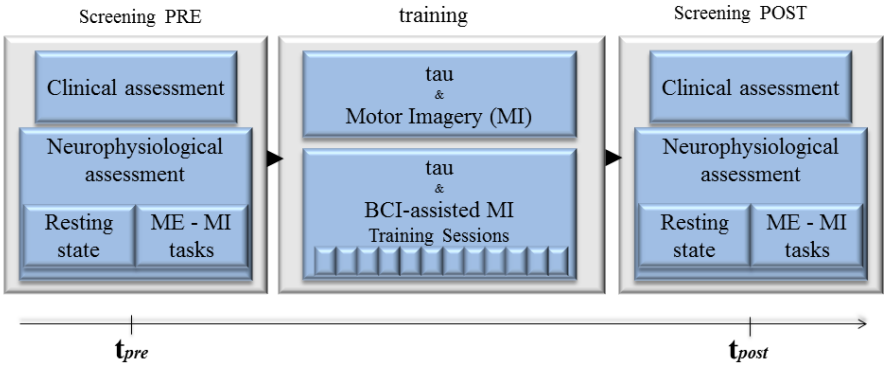

Figure 1.3. Rehabilitative protocol.

In all the applications described in the thesis, chronic patients (time from the event > 6 months) were excluded due to the different effects that a rehabilitative intervention can produce with respect to patients in subacute phase. In each application the patients' group (BCI and/or CTRL) and the subjects amount are specified: in fact as the PhD lasted three years, the amount of subjects enrolled in the study is different in the applications.

1.3 Training data

1.3.1 Experimental design

Twenty stroke patients (age: 62.9 ± 8.6 years) underwent the BCI–assisted MI training. The training was preceded and followed by two screening sessions (PRE, POST): data from screening PRE were used to

choose control features for BCI control. The features were spatially selected by a neurologist over the damaged hemisphere (two channels) at frequency ranges typical of sensorimotor rhythms (10-15 Hz). The protocol included 4 weeks of MI-based BCI training (3 sessions per week), during which the patient was asked to control the movements of a virtual representation of his own stroke-affected hand throughout MI tasks (grasping and complete finger extension). In particular Figure 1.4 shows the prototype setting for the BCI training sessions: the patient is seated with his hands resting on a desk, with an adjustable forearm orthosis that provide support. The hands are covered by a white blanket, on which a visual representation of the patient's hands ("virtual hands") are projected. During the session, the therapist is allowed to monitor the patient's mental "activity" continuously through on-line brain–computer interface feedback, displayed on a dedicated screen. The degree of desynchronization of selected features (electrodes and frequencies) determines the vertical velocity of the cursor on the therapist's screen; once the cursor reaches a target in the upper part of the screen, the virtual hand performs the imagined movement (feedback to patients in successful trials).

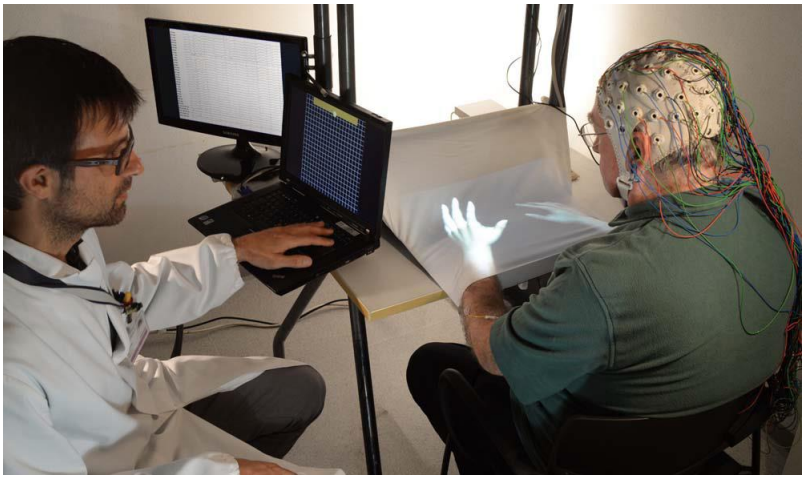

Figure 1.4. Prototype setting for the BCI training session.

1.3.2 Signals Processing

EEG signals were collected from 31 positions (frontocentral, central, centroparietal and parietal lines), sampling rate 200 Hz. In order to assess the BCI training effects, 2 training sessions were analyzed for each subject: an "*EARLY*" session, namely the second session for all subjects and a *"LATE"* session corresponding to a session in the last week of training, selected according to patient's performance rate. After preprocessing – downsampling at 100 Hz, band pass filtering (1-45 Hz), artifact rejection, CAR (*Common Average Reference*) spatial filtering – the power spectral densities (PSD) of the task- and baseline- related EEG signals were computed by means of the Welch method (Welch, 1967) and averaged within five frequency bands defined according to Individual Alpha Frequency (IAF, 9.7±0.5 Hz) (Klimesch, 1999):

- theta [IAF-6;IAF-2];
- alpha [IAF-2;IAF+2];
- beta1 [IAF+2;IAF+11];
- beta2 [IAF+11;IAF+20];
- gamma [IAF+20;IAF+35].

To highlight spectral activity related to the task, a statistical comparison (Student's t-test) for a significance level of 5% was computed between MI and baseline PSDs for each channel, frequency band and session (EARLY, LATE). Such test returned negative t-values in case of desynchronization (i.e. a decrease in power during task execution with respect to baseline phase) and positive t-value in case of synchronization (i.e. an increase in power). False Discovery Rate correction for multiple comparisons was applied to the statistical tests to avoid the occurrence of type I errors. In this way, we obtained statistical scalp maps (MI vs baseline) at each frequency band, for each session (EARLY, LATE), at single patient level.

To evaluate the efficacy of the BCI–assisted MI training and its consistency across patients, a statistical comparison (paired-sample t-test, significance level of 0.05) between negative t-values (associated to the desynchronizations) of EARLY and LATE sessions was performed for each channel and frequency band: the performed t-test is one-tailed in order to investigate a reinforcement of desynchronizations in LATE training session. FDR correction for multiple comparisons was applied to the statistical tests. Data from patients with lesion of the right hemisphere were flipped along the midsagittal plane, so that for group analysis, the ipsilesional side was common to all patients (De Vico Fallani et al. 2013; Luft et al. 2004; Ward et al. 2004). In this way, we obtained a statistical map of LATE vs EARLY, in each frequency band, at group level.

1.3.3 Results

Statistical scalp maps (MI vs baseline) for a representative patient in alpha and beta1 bands for EARLY and LATE sessions are reported in Figure 1.5. The color of each pixel codes for the correspondent t-value: gray for not significant differences, hot (yellow-red) and cold (blue) color scales for the level of significant synchronization and desynchronization, respectively. In the EARLY session, the pattern elicited in both bands is bilateral and *t* values are just above threshold. In the LATE session, higher involvement of the affected hemisphere (AH) was observed mainly in beta1 band. In fact, an increase of spectral desynchronization was visible in both frequency bands (absolute *t* values are greater than 10), mainly on the affected hemisphere. A similar sensory-motor rhythms (SMR) reactivity was observed in all patients.

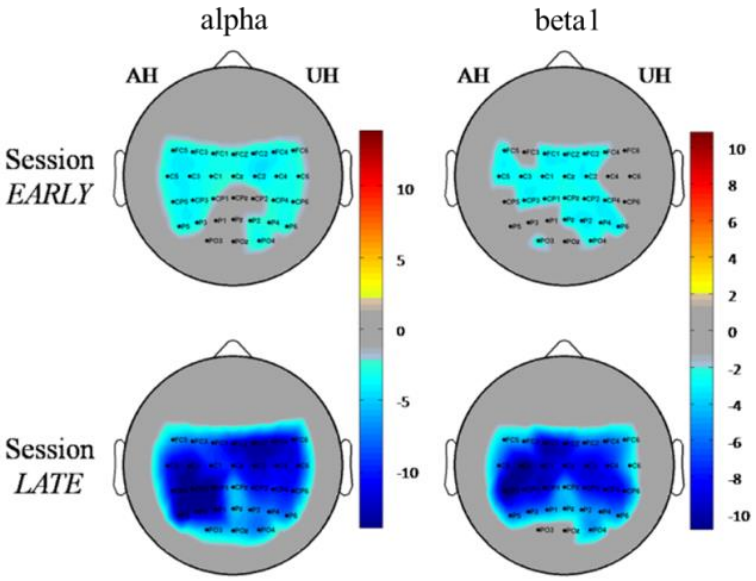

Figure 1.5. Statistical scalp maps of a subacute stroke patient: MI vs baseline in alpha and lower beta bands for the EARLY and LATE training sessions. Unaffected and Affected Hemisphere (UH; AH) are represented on the right and left of each scalp map, respectively. Color bars code for t-values.

Statistical group analysis related to the investigation of SMR pattern reinforcement, were performed considering only subacute patients (17 subjects). Figure 1.6 shows the obtained results mapped on a scalp model: significant differences associated to a reinforcement of the desynchronizations were found in alpha and beta1 bands. Statistical map in alpha band revealed significant activations at FC1, FC5, POz, PO4 electrodes, whereas beta1 map shows a large number of statistical differences especially above the affected hemisphere: these results show that the desynchronizations associated to LATE training session are stronger than those associate to the EARLY session in alpha and especially in beta1 bands.

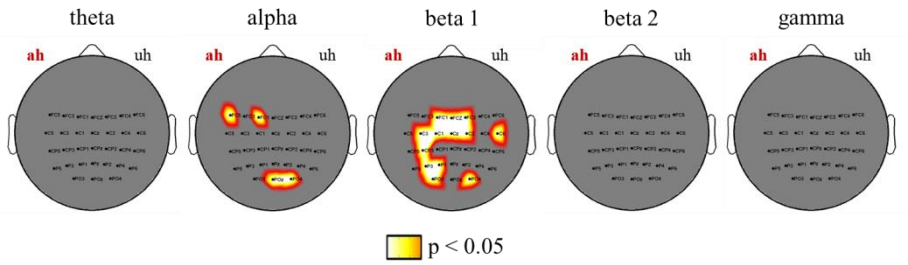

Figure 1.6. Maps of p values achieved from the statistical comparison LATE vs EARLY training sessions for BCI patients. The scalp model seen from above with the nose pointing to the upper part of the page, affected hemisphere (ah) is shown on the left side of the scalp in according with the flipping performed on data from patients with right lesion. The color of each pixel codes for the correspondent p-value: gray-red for not significant differences, whereas white-yellow for p-values below the threshold (corrected with FDR method)..

1.3.4 New indices for the quantification of specific features of the spectral activity

1.3.4.1 Global Power Hemisphere index

A new spectral index was defined in order to extract a quantifiable measure able to summarize the maps information and quantify the entity of the desynchronization in a specific scalp region. It is based on the spectral properties of the investigated conditions, called *Global Power Hemisphere* and defined as the sum of the negative t-values (t^-) resulted for the comparison between task and baseline PSDs for all EEG channels belonging to one hemisphere (*nCh*):

$$GlobPower_{Hem} = \sum_{i=1}^{nCh} t^-(i) \tag{1.1}$$

In according to equation (1.1), lower is the index value, stronger is the desynchronizazion. Similar indices can be defined to summarize the activity in other scalp macro-areas (ROIs) depending on the specific application.

Application of the new index and results

The *Global Power Hemisphere* index was applied to stroke patients data related to EARLY and LATE sessions with the aim to quantify the reinforcement of desynchronization elicited during MI task. For each subject, it was computed for each hemisphere, frequency band and session. Then a statistical comparison (paired-sample t-test, significance level of 0.05) was computed between the index extracted from the affected hemisphere and the unaffected one. Results obtained in beta1 band are shown in Figure 1.7: a significant difference between the affected and unaffected hemispheres was obtained only in LATE session (Fig.1.7-b). The other frequency bands showed the same behavior, thus revealing a higher involvement of the affected hemisphere in the MI execution at the end of the training (LATE session).

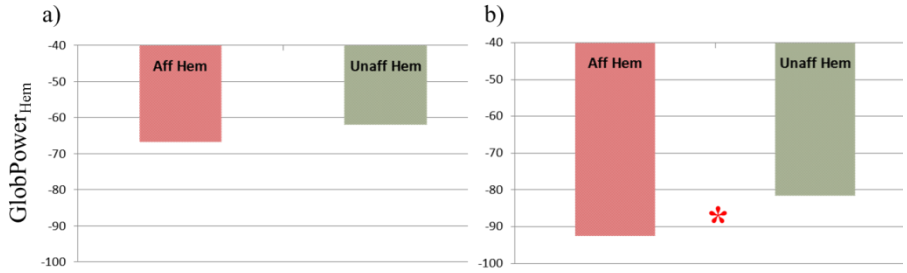

Figure 1.7. Paired-sample t-test computed between the GobPower$_{Hem}$ extracted from the affected and the unaffected hemisphere in EARLY session (panel a) and LATE session (panel b), with reference to beta1 band. Significant results ($p<0.05$) are highlighted with an asterisk.

1.3.4.2 A new descriptor of neuroelectrical activity during BCI–assisted MI training

An offline analysis on data acquired from stroke patients during all the training sessions was performed in order to define an index capable to monitor EEG patterns selected for BCI control across sessions, more appropriately than the usually adopted hit rate.

After EEG signals pre-processing (1-60 Hz band-pass and 50 Hz Notch filters, CAR spatial filtering) and PSD computation, a new index *h* was defined with the aim to describe the activity associated to the selected features, elicited during each trial. The index is defined as follows:

$$h = \alpha * t(ch_1, bin) + \beta * t(ch_2, bin) \quad (1.2)$$

where channels ch_1 and ch_2 and *bin* (2Hz-frequency range) are the features selected during the initial screening for each subject, α and β are multiplicative constants ($\alpha+\beta=1$), while *t* is the result of the Student's t test performed, for each trial, between the values of the PSD associated to the samples of task phase and those of baseline phase. The constants α and β allow to weigh in a different way the contributions from the two channels, but in this study they were set to the same value ($\alpha=\beta=0.5$).

The index *h* was calculated for each trial of the 12 sessions. For each session it was then possible to build the distribution of *h*. The median of the obtained distributions was used as a synthetic descriptor of the features, that was used to monitor the rehabilitative intervention session by session.

After the first overall assessment of the *h* distributions by means of the median, three percentiles of each distribution: 25% (first quartile), 50% (median) and 75% (last quartile) were investigated. This step was aimed to understand how trials are distributed according to the parameter *h*. By considering each percentile, the trials were divided into two groups, based on the value of the index *h*. The first group included trials for which *h* was smaller than the threshold associated to the percentile under examination, while the second included all the others.

After dividing the trials in the two groups, the statistical scalp maps associated to the trained 2Hz-frequency range was computed. These maps were obtained with Student's t-test on trials (significance level 5%) computed between MI and baseline PSDs. False Discovery Rate correction

for multiple comparisons was applied to the statistical tests to avoid the occurrence of type I errors (Benjamini and Yekutieli 2001). This procedure allowed to highlight spectral activity related to the task during selected trials.

Results

In Figure 1.8 the results obtained with EEG data acquired from a representative stroke patient (left affected hemisphere) are shown. The features selected for this patient are:

- channels: C3, Cp3;
- frequency bin: 10-12 Hz.

For each training session, index *h* was computed for each trial and a histogram was constructed. The first evaluation of the distributions obtained was performed by means of the median. In Figure 1.8, the trend of the median is shown as a function of training sessions. A comparison with the correspondent hit rate across sessions is also provided.

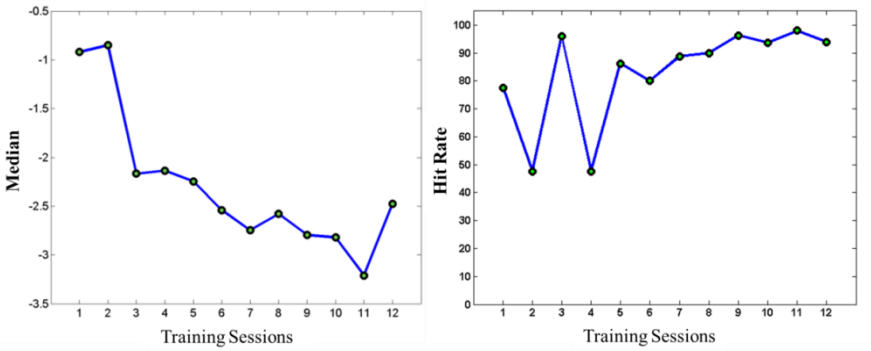

Figure 1.8. Median value of *h* and hit rate as a function of training sessions.

To understand how the trials were distributed with respect to the investigated measure, three percentiles (the first quartile, the median and the third quartile) were studied. The results obtained for the median in the second session are shown in Figure 1.9. The scalp map obtained with trials distributed to the left of median (i.e. stronger desynchronization) shows a significant pattern, while the scalp map on the right does not reveal

significant activations. The other percentiles have not shown the same performance.

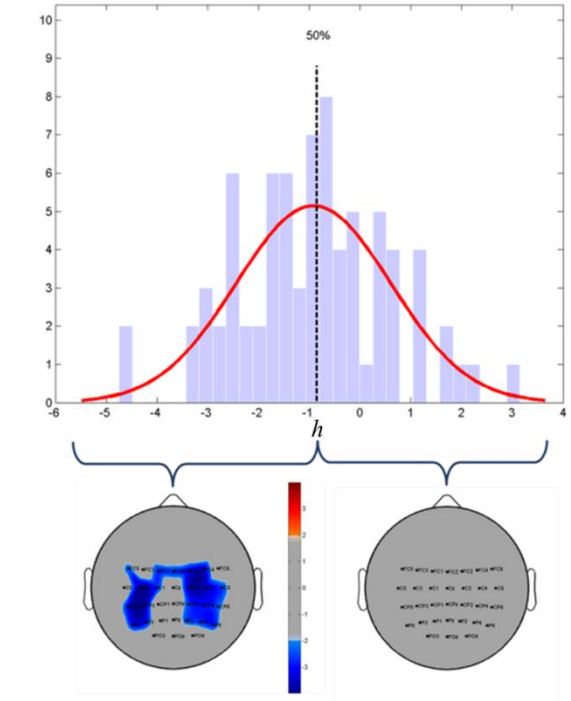

Figure 1.9: On the top the distribution of index *h* for an early session is shown, dashed line indicates the median (percentile 50%). On the bottom statistical scalp maps obtained with trials distributed to the left and to the right of the median. The color of each pixel codes for the correspondent t-value: gray for not significant differences, hot (yellow-red) and cold (blue) color scales for the level of significant synchronization and desynchronization, respectively. The two maps are related to the trained 2Hz-frequency range (10-12 Hz).

1.4 Screening data

1.4.1 Experimental groups

Two intervention groups were used for the evaluation of the more generalized effects of BCI-supported training on brain activity during MI task:

- BCI group (17 subjects): experimental patients group that received 1 month of "BCI-supported" MI training with 3 weekly sessions
- CTRL group (14 subjects): control patients group that received equally intensive MI training with no BCI assistance.

Chronic patients (time from the event > 6 months) were excluded from the study.

1.4.2 Signals Processing

EEG signals were collected from 61 positions during PRE and POST screening sessions. EEG data were downsampled at 100 Hz and bandpass filtered (1–45 Hz). Ocular artifacts were removed by Independent Component Analysis (ICA) and residual artifacts (muscular, environmental, etc) were removed using a semiautomatic procedure, based on the definition of a voltage threshold (±80 μV). The preprocessed EEG signals were then segmented, considering the last 4 seconds of each MI and rest trial as the period of interest (see Figure 1.1). After CAR spatial filtering, the PSDs of the task- and baseline- related EEG signals were computed and averaged within the five frequency bands defined according to IAF (as described in Training Study - *Signal Processing*). Thereafter, statistical PSD maps were generated for each patient's data set (MI task vs baseline), as performed in the training study (*Signal Processing* section).

To evaluate any significant differences in EEG reactivity at specific rhythms and brain areas between BCI and CTRL patients during the PRE and POST conditions, an independent two-sample t-test (significance level of 0.05) was performed using t-values obtain at the single-subject level (MI task vs baseline PSDs) and considering patients as repetitions. Bonferroni correction for multiple comparisons was applied to avoid the occurrence of type I errors (Bonferroni, 1936).

1.4.3 Results

As shown in Figure 1.10 (left panel), no significant differences were seen between the BCI and CTRL groups in desynchronized activity that was related to MI of the affected (paralyzed) hand in the PRE condition in any frequency band. In contrast, under the POST training conditions, a significantly more robust desynchronization ($p<0.05$, Bonferroni corrected) was reveled in the BCI versus CTRL group in the alpha and beta1 bands. These significant differences characterize only to the centroparietal regions of the ipsilesional hemisphere (ie, CP5 and CP3 electrodes; see Fig 10, left panel, lower row) and the central midline (Cz electrode) in the alpha oscillatory band. At the higher frequency (beta1), these differences still involved mainly the ipsilesional hemisphere (C1, CP1), but C2 (contralesional hemisphere) and Cz electrodes were also involved (see Fig 10, left panel, lower row).

Similar to what was observed for the MI task of the paralyzed hand, the MI task with the unaffected hand was not associated with significant differences in the PRE screening session. In the POST training condition, however, there was a significant difference (BCI>CTRL; $p<0.05$, Bonferroni corrected) only over the contralesional hemisphere (C4 and FC2 electrodes) in the alpha and beta1 bands (see Fig 1.10, right panel, lower row).

Any significant differences were found in synchronization patterns that were related to affected and unaffected hand grasping MI in PRE or POST training.

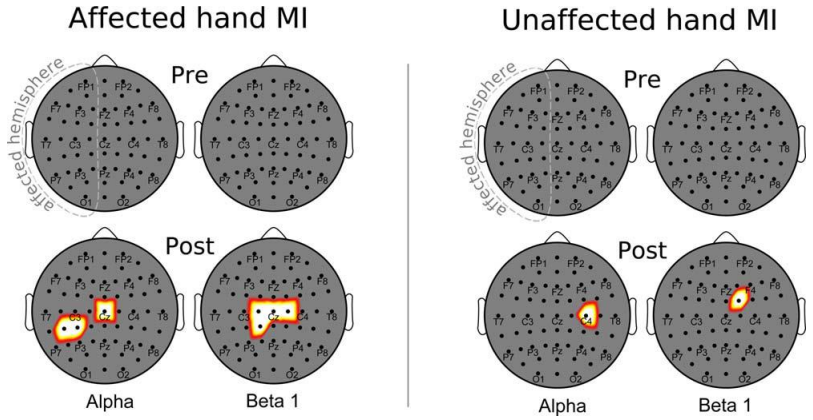

Figure 1.10: Statistical scalp maps associated with grasping movement imagery of the affected (left panel) and unaffected (right panel) hands. t Tests were performed to analyze the desynchronization between the brain–computer interface (BCI) and control (CTRL) groups in the PRE (upper row) and POST (lower row) sessions in the alpha and beta1 frequency ranges. The scalp model is seen from above, with the nose pointing toward the upper part of the page, and the affected hemisphere is shown on the left side of the scalp. The color of each pixel represents the corresponding probability value. Gray indicates nonsignificant differences; white–yellow indicates stronger desynchronization ($p < 0.05$, Bonferroni corrected) in the BCI group; and black denotes stronger desynchronization ($p < 0.05$, Bonferroni corrected) in the CTRL group.

1.5 Discussion and conclusion

In the present section a description of methods for the evaluation of changes in brain activity was proposed. The application of these methods to the experimental subjects and protocol were described, showing the validity of the procedure that can be applied in a wide range of applications (e.g. evaluation of therapy effects, assessment of brain functions recovery,…).

In the application under investigation, statistical within-group (BCI patients) analysis was performed in order to evaluate a possible reinforcement of desynchronization between the two sessions of the BCI-assisted MI training (EARLY and LATE). Indeed, resulting statistical maps showed that the desynchronizations associated to LATE training session are stronger than those associated to the EARLY session in a selective way for

the trained rhythms (alpha and beta bands) and in specific locations (statistical differences especially above the affected hemisphere). This result indicates that the statistical maps can be an appropriate index to localize the effects of a treatment in a group analysis. Furthermore the application of the same procedure to screening data allows to perform a between-groups study. The obtained results highlight the value of the BCI closed loop in facilitating greater "physiological" recruitment of the stroke-affected hemisphere with respect to MI practice without feedback.

Furthermore some methodological developments were proposed here.

The spectral index, described in section "*Definition of indices based on the spectral activity"*, was used to quantify the differences in desynchronization between the two hemispheres in EARLY and LATE sessions in the BCI group by means of statistical comparisons. Results of the tests showed that in EARLY session there were no significant differences indicating that patterns elicited are bilateral, whereas in LATE session significant difference was revealed indicating a higher involvement of the affected hemisphere during the task execution, as a result of the training. The proposed index thus proved useful to unveil a specific effect of the rehabilitation intervention in a statistical and quantifiable way.

Furthermore, a new index was defined as a function of features selected for the training of motor imagery as a rehabilitative intervention after stroke. This measure in associated to the signals acquired from electrodes positioned over the damage hemisphere and to the frequency ranges typical of sensorimotor rhythms. In particular it is function of the value of *t* obtained for each trial with a Student's t test between samples associated to MI-task execution and baseline phase samples. This value is therefore a measure of the desynchronization elicited by the patient. The *h* distribution associated to each session allowed to evaluate how the trials are distributed with respect to the index. The median of the distributions proved to be more stable than the

hit rate as a descriptor of the trend of the training sessions, and it suggested an increase of spectral desynchronization associated to the MI task execution. The statistical scalp maps obtained from the trials to the left of the median provided a topological description of the activation underlying the execution of "good" trials, which is in agreement with the physiology of the trained function. It was possible to achieve such result from the very early sessions thanks to the use of the *h* index.

The preliminary results suggest that the proposed procedure may have a future role in helping to understand the neuroplasticity at the basis of a neurofeedback based training and in optimizing a BCI based intervention for neurorehabilitation.

All the described analyses converge toward similar results and conclusions: a stronger involvement of the affected hemisphere was observed across training, possibly reflecting a motor cortex functional recruitment bringing closer to normal, as disclosed by EEG patterns elicited by MI in a BCI context. How this increased motor-related brain activity can impact on the actual functional motor recovery of subacute patients remains to be elucidated. Functional neuroimaging brain maps reveal where the cortical activations appear during the execution of a task: more interesting results could be provided investigating how the cerebral areas involved in a task cooperate for its execution and how this communication is modulated by a rehabilitative treatment for the study of the possible recovery of a damaged brain function (*plasticity phenomena*).

Section I References

Akaike, H. 1974. “A New Look at Statistical Model Identification.” *IEEE Trans Automat Control* 19: 716–23.

Astolfi, Laura, Febo Cincotti, Donatella Mattia, M G Marciani, Luis A Baccalà, Fabrizio de Vico Fallani, Serenella Salinari, Mauro Ursino, Melissa Zavaglia, and Fabio Babiloni. 2006. “Assessing Cortical Functional Connectivity by Partial Directed Coherence: Simulations and Application to Real Data.” *IEEE Transactions on Bio-Medical Engineering* 53 (9): 1802–12. doi:10.1109/TBME.2006.873692.

Astolfi, Laura, Febo Cincotti, Donatella Mattia, M Grazia Marciani, Luiz A Baccala, Fabrizio de Vico Fallani, Serenella Salinari, et al. 2007. “Comparison of Different Cortical Connectivity Estimators for High-Resolution EEG Recordings.” *Hum Brain Mapp* 28 (2): 143–57. doi:10.1002/hbm.20263.

Baccalá, Luiz A., and Koichi Sameshima. 2001. “Partial Directed Coherence: A New Concept in Neural Structure Determination.” *Biological Cybernetics* 84 (6): 463–74. doi:10.1007/PL00007990.

Benjamini, Yoav, and Daniel Yekutieli. 2001. “The Control of the False Discovery Rate in Multiple Testing under Dependency.” *The Annals of Statistics* 29 (4): 1165–88.

Blinowska, Katarzyna J. 2011. “Review of the Methods of Determination of Directed Connectivity from Multichannel Data.” *Medical & Biological Engineering & Computing* 49 (5): 521–29. doi:10.1007/s11517-011-0739-x.

Bonferroni, Carlo Emilio. 1936. *Teoria statistica delle classi e calcolo delle probabilità*. Libreria internazionale Seeber.

Cicinelli, Paola, Barbara Marconi, Marina Zaccagnini, Patrizio Pasqualetti, Maria Maddalena Filippi, and Paolo Maria Rossini. 2006. “Imagery-Induced Cortical Excitability Changes in Stroke: A Transcranial Magnetic Stimulation Study.” *Cerebral Cortex (New York, N.Y.: 1991)* 16 (2): 247–53. doi:10.1093/cercor/bhi103.

Cramer, Steven C., Mriganka Sur, Bruce H. Dobkin, Charles O’Brien, Terence D. Sanger, John Q. Trojanowski, Judith M. Rumsey, et al. 2011. “Harnessing Neuroplasticity for Clinical Applications.” *Brain: A Journal of Neurology* 134 (Pt 6): 1591–1609. doi:10.1093/brain/awr039.

De Vico Fallani, Fabrizio, Floriana Pichiorri, Giovanni Morone, Marco Molinari, Fabio Babiloni, Febo Cincotti, and Donatella Mattia. 2013. “Multiscale Topological Properties of Functional Brain Networks during Motor Imagery after Stroke.” *NeuroImage* 83 (December): 438–49. doi:10.1016/j.neuroimage.2013.06.039.

Dimyan, Michael A., and Leonardo G. Cohen. 2011. “Neuroplasticity in the Context of Motor Rehabilitation after Stroke.” *Nature Reviews. Neurology* 7 (2): 76–85. doi:10.1038/nrneurol.2010.200.

Efron, B. 1979. “Bootstrap Methods: Another Look at the Jackknife.” *The Annals of Statistics* 7 (1): 1–26. doi:10.1214/aos/1176344552.

———. 1982. *The Jackknife, the Bootstrap and Other Resampling Plans*. CBMS-NSF Regional Conference Series in Applied Mathematics. Society for Industrial and Applied Mathematics. http://epubs.siam.org/doi/book/10.1137/1.9781611970319.

Friston, K. J., C. D. Frith, and R. S. J. Frackowiak. 1993. “Time-Dependent Changes in Effective Connectivity Measured with PET.” *Human Brain Mapping* 1 (1): 69–79. doi:10.1002/hbm.460010108.

Gaggioli, Andrea, Andrea Meneghini, Francesca Morganti, Mariano Alcaniz, and Giuseppe Riva. 2006. “A Strategy for Computer-Assisted Mental Practice in Stroke Rehabilitation.” *Neurorehabilitation and Neural Repair* 20 (4): 503–7. doi:10.1177/1545968306290224.

Granger, C. W. J. 1969. “Investigating Causal Relations by Econometric Models and Cross-Spectral Methods.” *Econometrica* 37 (3): 424–38. doi:10.2307/1912791.

Guo, Xiaoli, Zheng Jin, Xinyang Feng, and Shanbao Tong. 2014. “Enhanced Effective Connectivity in Mild Occipital Stroke Patients With Hemianopia.” *IEEE Transactions on Neural Systems and Rehabilitation Engineering* 22 (6): 1210–17. doi:10.1109/TNSRE.2014.2325601.

Hanakawa, Takashi, Michael A. Dimyan, and Mark Hallett. 2008. “Motor Planning, Imagery, and Execution in the Distributed Motor Network: A Time-Course Study with Functional MRI.” *Cerebral Cortex (New York, N.Y.: 1991)* 18 (12): 2775–88. doi:10.1093/cercor/bhn036.

Horwitz, Barry. 2003. “The Elusive Concept of Brain Connectivity.” *NeuroImage* 19 (2 Pt 1): 466–70.

Ietswaart, Magdalena, Marie Johnston, H. Chris Dijkerman, Sara Joice, Clare L. Scott, Ronald S. MacWalter, and Steven J. C. Hamilton. 2011. “Mental Practice with Motor Imagery in Stroke Recovery: Randomized Controlled Trial of Efficacy.” *Brain: A Journal of Neurology* 134 (Pt 5): 1373–86. doi:10.1093/brain/awr077.

Kaiser, Vera, Ian Daly, Floriana Pichiorri, Donatella Mattia, Gernot R. Müller-Putz, and Christa Neuper. 2012. “Relationship between Electrical Brain Responses to Motor Imagery and Motor Impairment in Stroke.” *Stroke; a Journal of Cerebral Circulation* 43 (10): 2735–40. doi:10.1161/STROKEAHA.112.665489.

Kaminski, M. J., and K. J. Blinowska. 1991. “A New Method of the Description of the Information Flow in the Brain Structures.” *Biological Cybernetics* 65 (3): 203–10. doi:10.1007/BF00198091.

Kelly, K.M., D.S. Shiau, R.T. Kern, J.H. Chien, M.C.K. Yang, K.A. Yandora, J.P. Valeriano, J.J. Halford, and J.C. Sackellares. 2010. “Assessment of a Scalp EEG-Based Automated Seizure Detection System.” *Clinical Neurophysiology : Official Journal of the International Federation of Clinical Neurophysiology* 121 (11): 1832–43. doi:10.1016/j.clinph.2010.04.016.

Klimesch, W. 1999. “EEG Alpha and Theta Oscillations Reflect Cognitive and Memory Performance: A Review and Analysis.” *Brain Research. Brain Research Reviews* 29 (2-3): 169–95.

Kuś, Rafal, Maciej Kamiński, and Katarzyna J. Blinowska. 2004. “Determination of EEG Activity Propagation: Pair-Wise versus Multichannel Estimate.” *IEEE Transactions on Bio-Medical Engineering* 51 (9): 1501–10. doi:10.1109/TBME.2004.827929.

Liu, Karen P. Y., Chetwyn C. H. Chan, Rebecca S. M. Wong, Ivan W. L. Kwan, Christina S. F. Yau, Leonard S. W. Li, and Tatia M. C. Lee. 2009. “A Randomized Controlled Trial of Mental Imagery Augment Generalization of Learning in Acute Poststroke Patients.” *Stroke; a Journal of Cerebral Circulation* 40 (6): 2222–25. doi:10.1161/STROKEAHA.108.540997.

Luft, Andreas R., Sandy Waller, Larry Forrester, Gerald V. Smith, Jill Whitall, Richard F. Macko, Jörg B. Schulz, and Daniel F. Hanley. 2004. “Lesion Location Alters Brain Activation in Chronically Impaired Stroke Survivors.” *NeuroImage* 21 (3): 924–35. doi:10.1016/j.neuroimage.2003.10.026.

Malouin, Francine, and Carol L. Richards. 2010. “Mental Practice for Relearning Locomotor Skills.” *Physical Therapy* 90 (2): 240–51. doi:10.2522/ptj.20090029.

Meyer, Joseph S., Christopher G. Ingersoll, Lyman L. McDonald, and Marks S. Boyce. 1986. “Estimating Uncertainty in Population Growth Rates: Jackknife vs. Bootstrap Techniques.” *Ecology* 67 (5): 1156–66. doi:10.2307/1938671.

Murias, Michael, Sara J. Webb, Jessica Greenson, and Geraldine Dawson. 2007. “Resting State Cortical Connectivity Reflected in EEG Coherence in Individuals with Autism.” *Biological Psychiatry* 62 (3): 270–73. doi:10.1016/j.biopsych.2006.11.012.

Page, Stephen J., Peter Levine, and Anthony Leonard. 2007. “Mental Practice in Chronic Stroke: Results of a Randomized, Placebo-Controlled Trial.” *Stroke; a Journal of Cerebral Circulation* 38 (4): 1293–97. doi:10.1161/01.STR.0000260205.67348.2b.

Petti, M., S. Caschera, A. Anzolin, J. Toppi, F. Pichiorri, F. Babiloni, F. Cincotti, D. Mattia, and L. Astolfi. 2015. “Effect of Inter-Trials Variability on the Estimation of Cortical Connectivity by Partial Directed Coherence.” In *2015 37th Annual International Conference of the IEEE Engineering in Medicine and Biology Society (EMBC)*, 3791–94. doi:10.1109/EMBC.2015.7319219.

Petti, M., F. Pichiorri, J. Toppi, F. Cincotti, S. Salinari, F. Babiloni, D. Mattia, and L. Astolfi. 2014. “Individual Cortical Connectivity Changes after Stroke: A Resampling Approach to Enable Statistical Assessment at Single-Subject Level.” In , 2785–88. IEEE. doi:10.1109/EMBC.2014.6944201.

Pfurtscheller, G., and F. H. Lopes da Silva. 1999. “Event-Related EEG/MEG Synchronization and Desynchronization: Basic Principles.” *Clinical Neurophysiology: Official Journal of the International Federation of Clinical Neurophysiology* 110 (11): 1842–57.

Pichiorri, F., F. De Vico Fallani, F. Cincotti, F. Babiloni, M. Molinari, S. C. Kleih, C. Neuper, A. Kübler, and D. Mattia. 2011. “Sensorimotor Rhythm-Based Brain-Computer Interface Training: The Impact on Motor Cortical Responsiveness.” *Journal of Neural Engineering* 8 (2): 025020. doi:10.1088/1741-2560/8/2/025020.

Pichiorri, Floriana, Giovanni Morone, Manuela Petti, Jlenia Toppi, Iolanda Pisotta, Marco Molinari, Stefano Paolucci, et al. 2015. “Brain-Computer Interface Boosts Motor Imagery Practice during Stroke Recovery: BCI and Motor Imagery.” *Annals of Neurology* 77 (5): 851–65. doi:10.1002/ana.24390.

Rotondi, Fabio, Silvana Franceschetti, Giuliano Avanzini, and Ferruccio Panzica. 2015. “Altered EEG Resting-State Effective Connectivity in Drug-Naïve Childhood Absence Epilepsy.” *Clinical Neurophysiology*. Accessed November 18. doi:10.1016/j.clinph.2015.09.003.

Sakoğlu, Ünal, Godfrey D. Pearlson, Kent A. Kiehl, Y. Michelle Wang, Andrew M. Michael, and Vince D. Calhoun. 2010. “A Method for Evaluating Dynamic Functional Network Connectivity and Task-Modulation: Application to Schizophrenia.” *Magma (New York, N.Y.)* 23 (5-6): 351–66. doi:10.1007/s10334-010-0197-8.

Sameshima, K., and L. A Baccalá. 1999. “Using Partial Directed Coherence to Describe Neuronal Ensemble Interactions.” *Journal of Neuroscience Methods* 94 (1): 93–103.

Shao, Jun, and Dongsheng Tu. 2012. *The Jackknife and Bootstrap*. Springer Science & Business Media.

Sharma, Nikhil, and Jean-Claude Baron. 2013. “Does Motor Imagery Share Neural Networks with Executed Movement: A Multivariate fMRI

Analysis." *Frontiers in Human Neuroscience* 7: 564. doi:10.3389/fnhum.2013.00564.

Sharma, Nikhil, Jean-Claude Baron, and James B. Rowe. 2009. "Motor Imagery after Stroke: Relating Outcome to Motor Network Connectivity." *Annals of Neurology* 66 (5): 604–16. doi:10.1002/ana.21810.

Shih, Jerry J., Dean J. Krusienski, and Jonathan R. Wolpaw. 2012. "Brain-Computer Interfaces in Medicine." *Mayo Clinic Proceedings* 87 (3): 268–79. doi:10.1016/j.mayocp.2011.12.008.

Stephen, Emily P., Kyle Q. Lepage, Uri T. Eden, Peter Brunner, Gerwin Schalk, Jonathan S. Brumberg, Frank H. Guenther, and Mark A. Kramer. 2014. "Assessing Dynamics, Spatial Scale, and Uncertainty in Task-Related Brain Network Analyses." *Frontiers in Computational Neuroscience* 8 (March). doi:10.3389/fncom.2014.00031.

Takahashi, Daniel Yasumasa, Luis A. Baccalà, and Koichi Sameshima. 2007. "Connectivity Inference between Neural Structures via Partial Directed Coherence." *Journal of Applied Statistics* 34 (10): 1259–73. doi:10.1080/02664760701593065.

Toppi, J., A. Anzolin, M. Petti, F. Cincotti, D. Mattia, S. Salinari, F. Babiloni, and L. Astolfi. 2014. "Investigating Statistical Differences in Connectivity Patterns Properties at Single Subject Level: A New Resampling Approach." In *Engineering in Medicine and Biology Society (EMBC), 2014 36th Annual International Conference of the IEEE*, 6357–60. IEEE. http://ieeexplore.ieee.org/xpls/abs_all.jsp?arnumber=6945082.

Toppi, J., F. De Vico Fallani, G. Vecchiato, A. G. Maglione, F. Cincotti, D. Mattia, S. Salinari, F. Babiloni, and L. Astolfi. 2012. "How the Statistical Validation of Functional Connectivity Patterns Can Prevent Erroneous Definition of Small-World Properties of a Brain Connectivity Network." *ComputatComputational and Mathematical Methods in Medicine* 2012 (August): e130985. doi:10.1155/2012/130985, 10.1155/2012/130985.

Tukey, John Wilder. 1958. "Bias and Confidence in Not Quite Large Samples." *The Annals of Mathematical Statistics* 29 (2): 614–23. doi:10.1214/aoms/1177706647.

Turbes, C. C., G. T. Schneider, and R. J. Morgan. 1983. "Partial Coherence Estimates of Brain Rhythms." *Biomedical Sciences Instrumentation* 19: 97–102.

Van Meer, Maurits P. A., Kajo van der Marel, Kun Wang, Willem M. Otte, Soufian El Bouazati, Tom A. P. Roeling, Max A. Viergever, Jan Willem Berkelbach van der Sprenkel, and Rick M. Dijkhuizen. 2010. "Recovery of Sensorimotor Function after Experimental

Stroke Correlates with Restoration of Resting-State Interhemispheric Functional Connectivity." *The Journal of Neuroscience: The Official Journal of the Society for Neuroscience* 30 (11): 3964–72. doi:10.1523/JNEUROSCI.5709-09.2010.

Varotto, Giulia, Patrik Fazio, Davide Rossi Sebastiano, Dunja Duran, Ludovico D'Incerti, Eugenio Parati, Davide Sattin, Matilde Leonardi, Silvana Franceschetti, and Ferruccio Panzica. 2014. "Altered Resting State Effective Connectivity in Long-Standing Vegetative State Patients: An EEG Study." *Clinical Neurophysiology* 125 (1): 63–68. doi:10.1016/j.clinph.2013.06.016.

Ward, Nick S., Martin M. Brown, Alan J. Thompson, and Richard S. J. Frackowiak. 2004. "The Influence of Time after Stroke on Brain Activations during a Motor Task." *Annals of Neurology* 55 (6): 829–34. doi:10.1002/ana.20099.

Welch, Peter D. 1967. "The Use of Fast Fourier Transform for the Estimation of Power Spectra: A Method Based on Time Averaging over Short, Modified Periodograms." *IEEE Transactions on Audio and Electroacoustics* 15 (2): 70–73. doi:10.1109/TAU.1967.1161901.

Wolpaw, Jonathan R., Niels Birbaumer, Dennis J. McFarland, Gert Pfurtscheller, and Theresa M. Vaughan. 2002. "Brain-Computer Interfaces for Communication and Control." *Clinical Neurophysiology: Official Journal of the International Federation of Clinical Neurophysiology* 113 (6): 767–91.

Section II

Assessing changes in brain connectivity

2.1 Introduction

In Neuroscience, the concept of brain connectivity is crucial to understand how communication between cortical regions is organized. Brain connectivity can be estimated from a wide range of biomedical signals and with different methods. Several definitions have been provided to describe the information returned by such methods, depending on data characteristics and on approaches used for the investigation of cerebral processes. Specifically, *effective connectivity* aims at describing the influence of one neural system over another in the form of connectivity patterns indicating direction and strength of the information flow between such systems (Friston, Frith, and Frackowiak 1993; Horwitz 2003).

Brain connectivity estimation based on EEG data has many advantages related to the nature of these signals: high temporal resolution, noninvasiveness and low-cost. An EEG setup can be used in a wide range of pathological conditions and can be easily adapted to different clinical settings. From EEG signals recorded on the scalp, effective connectivity can be estimated using methods based on Granger causality (Granger 1969)

which are defined both in time and in frequency domain (Blinowska 2011; Kaminski and Blinowska 1991; Sameshima and Baccalá 1999; Turbes, Schneider, and Morgan 1983), and based on bivariate or multivariate autoregressive models that allow to reconstruct the direction of information flows. Among the Granger causality based methods, the frequency domain estimator Partial Directed Coherence (PDC) (Sameshima and Baccalá 1999) is based on multivariate autoregressive (MVAR) models built on original time-series (Kuś, Kamiński, and Blinowska 2004) and is known to be characterized by high accuracy in the estimation of connectivity patterns, distinguishing between direct and indirect connectivity flows better than other estimators (Astolfi et al. 2007).

Several studies proved that PDC technique is a powerful estimator of brain connectivity and it can be applied for the investigation of different cerebral functions in physiological and pathological conditions (Pichiorri et al. 2015; Rotondi et al. 2015; Guo et al. 2014; Varotto et al. 2014; Petti et al. 2015). All these studies performed group analyses, e.g. comparing a patients' population with a control group (between-groups analysis) or different experimental conditions (e.g. before and after a therapy) of the same population (within-group analysis). When the aim of the study is to evaluate the effects of a treatment, and thus the possible recovery of a damaged brain function (*plasticity phenomena*), group analysis is a powerful method to assess the consistent effects of a therapy. On the other hand, the diversity of each patient's conditions leads to a difficulty in building homogeneous experimental groups, and specific effects at the single patient level may be hidden. Moreover, assessing significant changes in the brain organization of a specific patient (for instance, as a consequence of a treatment) is of particular interest for clinical applications, for the possibility to perform correlation analysis with functional changes induced by the treatment (e.g. a rehabilitation intervention). The importance of a correct validation of

connectivity patterns before the computation of graph indices to describe their properties has recently been demonstrated (Toppi et al. 2012).

At the state of the art, the statistical evaluation of changes in brain connectivity at the single subject level is methodologically challenging, as PDC (as well as other multivariate estimators) requires a considerable amount of data to provide an accurate modeling of the network involving all the signals. In particular, to achieve a sufficient accuracy in the estimation, the amount of data has to be proportional to the complexity of the MVAR model needed to perform a fully multivariate analysis. Nevertheless, the advantage of multivariate approaches over bivariate ones (see for instance (Kuś, Kamiński, and Blinowska 2004)) has been proved, in terms of correct reconstruction of the brain network and consequently of its properties (as returned, for instance, by a graph theoretical analysis). To meet these requirements in terms of data amount, EEG experimental designs aimed at connectivity estimation are usually characterized by several repetitions of the experimental task in the same conditions, which leads to the collection of a multi-trials dataset. However, the estimation using the single trial data is not stable and accurate, and thus the amount of data that can be reasonably collected in an EEG session is entirely used to obtain an unique and accurate estimation. This prevents from performing multiple estimations of connectivity patterns in a single condition, and thus to obtain the distribution needed to perform a statistical comparison between conditions at a single subject level.

In the first part of this section, the state of the art methods for estimation and validation of the effective connectivity are explained. Then they were applied on EEG signals recorded at rest from stroke patients before and after a rehabilitative intervention and group analysis was performed to assess the consistent effects of the therapy with particular interest to the connectivity pattern that the subjects significantly reinforced after the training.

In the second part, several issues related to the brain connectivity estimation starting to multi-trials EEG dataset are investigated. In particular the main aim of the methodological developments described here is to provide a new statistical procedure to overcome the above-mentioned limitations in the statistical evaluation of brain connectivity changes at the single-subject level. The idea is to apply a resampling approach to multi-trials EEG data, generating a distribution of datasets in each single condition, to be then subjected to connectivity estimation. For this purpose, two resampling methods are here investigated: Bootstrap (Efron 1979) and Jackknife (Tukey 1958). The first approach consists of keeping constant the number of trials through the exclusion of some of them and the repetition of others, while Jackknife foresees a leave-N out approach on trials. Developed in statistics field for variance and bias estimation (Efron 1982), in the last decade both methods have been employed in Neuroscience literature with different aims, e.g. to establish confidence interval for graph network indices (Stephen et al. 2014; Toppi et al. 2014) or for validation purposes (Kelly et al. 2010; Sakoğlu et al. 2010; Murias et al. 2007). However, their use to compare different conditions at single subject level has not been proposed yet, and a systematic evaluation of their performances under different factors is still lacking.

To perform this kind of study, preliminary investigations have to be performed. Indeed a first observation is related to the assumption of stationarity of the data across the trials during an experimental session: this hypothesis cannot be easily guaranteed, due to many possible reasons (different signal-to-noise ratio; subjects' fatigue or lack of concentration; oscillations in the task performances, especially in the case of pathological subjects). The evaluation of inter-trials variability (ITV) effects on PDC accuracy is of general interest for all the possible applications and also here

is required because the use of a resampling approach on multi-trials EEG data can generate datasets with high ITV.

Once the robustness and the accuracy of PDC patterns has been proved, a second investigation is required in order to assess the properties of PDC distributions generated by the two resampling approaches (Petti et al. 2014).

Two ad hoc simulation studies were designed to investigate the two points above described, and as last step a simulation study was conducted in order to evaluate the performance obtained when two connectivity distributions are statistically compared. In particular, the specific aims of this last and more complex simulation study are the following:

1. to evaluate the accuracy of the statistical procedure proposed for the single-subject study;
2. to compare the Bootstrap and the Jackknife approaches;
3. to provide indications useful to select specific parameters and statistical tests, with the aim to maximize the accuracy of the procedure under different experimental conditions.

Once the performances of the different approaches were explored, the method characterized by higher accuracy was applied to real data. To this purpose, stroke patients EEG data recorded in two recording sessions (PRE and POST the BCI-assisted MI training) were used. In particular, for each patient, the brain connectivity pattern underlying the attempted movement of the affected hand (grasping) was compared before and after the intervention, with particular interest to the connectivity network that the subjects significantly reinforced after the training.

2.2 Methods: State of the Art in Connectivity Estimation

2.2.1 Multivariate Autoregressive Modeling of Brain Signals

Supposing that the following multivariate autoregressive (MVAR) model is an adequate description of the dataset Y:

$$\sum_{k=0}^{p} \Lambda(k) Y(t-k) = E(t) \tag{2.1}$$

where Y(t) is the data vector in time, E(t) is a vector of multivariate zero-mean uncorrelated white noise processes, Λ(k) is the matrix of model coefficients at lag k and p is the model order, that can be chosen by means of the Akaike Information Criteria (AIC) for MVAR processes (Akaike 1974). For the dataset used in this study, the resulting optimal model order was around 20 for each subject. We checked that the amount of data points was at least an order of magnitude higher than the number of parameters to be estimated for the model. In order to investigate the spectral properties of the examined process, (2.1) is transformed to the frequency domain:

$$\begin{aligned} &\Lambda(f) Y(f) = E(f), \\ &\Lambda(f) = \sum_{k=0}^{p} \Lambda(k) e^{-j 2\pi f \Delta t k} \end{aligned} \tag{2.2}$$

where Δt is the temporal interval between two samples.

2.2.2 Partial Directed Coherence

The PDC (Sameshima and Baccalá 1999) is a powerful estimator of effective connectivity, used to determine the directed influences between any given pair of signals in a multivariate data set. As a frequency-domain version of Granger causality (Granger 1969; Baccalá and Sameshima 2001), PDC reveals the existence, the direction and the strength of a functional

relationship between any given pair of signals in a multivariate data set; it can be defined as follows:

$$\pi_{ij}(f) = \frac{\Lambda_{ij}(f)}{\sqrt{\sum_{k=1}^{N} \Lambda_{ik}(f)\Lambda_{ik}(f)}} \tag{2.3}$$

where Λ(f) is the matrix containing the coefficients of associated MVAR model and:

$$\sum_{n=1}^{N} |\pi_{in}(f)|^2 = 1 \tag{2.4}$$

Due to the normalization reported in (2.4), PDC values are in the interval [0 1]. With respect to the original definition of PDC (Baccalá and Sameshima 2001), according to which the estimator is normalized according to the amount of connectivity emitted from the "source" channel, here we normalized the estimator according to the total connectivity incoming to the "target" channel (row-wise normalization instead of column-wise), to avoid that PDC from given electrode is decreased when multiple signals are emitted from it.

Moreover, a squared formulation of PDC has been introduced and can be defined as:

$$\pi_{ij}^{S}(f) = \frac{|\Lambda_{ij}(f)|^2}{\sum_{k=1}^{N} |\Lambda_{ik}(f)|^2} \tag{2.5}$$

The main difference with respect to the original formulation is in the interpretation of the estimator. Squared PDC can be put in relationship with the power density of the investigated signals and can be interpreted as the fraction of i^{th} signal power density due to the j^{th} measure. The higher performances of squared methods in respect to simple PDC have been demonstrated in a simulation study. Such study revealed higher accuracy, for

the methods based on squared formulation of PDC, in the estimation of connectivity patterns on data characterized by different lengths and signal to noise ratio (SNR) and in distinction between direct and indirect pathways (Astolfi et al. 2006).

2.2.3 Statistical Assessment of Connectivity Estimates

The assessment of the significance of the estimated causal links can be performed by means of asymptotic statistic method (Takahashi, Baccalà, and Sameshima 2007). Such method is based on the assumption that PDC tends to a Gaussian distribution in the non-null case and to a $\chi 2$ distribution in the null case. This validation approach, the asymptotic statistic, allowed to derive the probability distribution (the $\chi 2$ distribution) of a function of the null-case squared PDC estimator, knowing its asymptotic variance. The statistical threshold corresponds to the 95th percentile of this distribution.

2.2.4 Application to real EEG data: resting state

2.2.4.1 Methods

After preprocessing – downsampling at 100 Hz, band pass filtering (1-45 Hz), artifact rejection – effective connectivity was computed on EEG signals recorded at rest (resting state) during the PRE and POST screening sessions on a subgroup of BCI (n=11) and CTRL (n=9) patients. To reduce the computational complexity, PDC values were calculated from 51 of 61 EEG channels (omitting the most peripheral electrode leads: Fpz, AF7, AF8, FT7, FT8, TP7, TP8, PO7, PO8, and Oz) for each frequency band (theta, alpha, beta1, beta2, gamma; defined in Section I).

Once the connectivity estimation were obtained, the study focused on the interhemispheric connections (IHCs), based on evidence that changes in connectivity between hemispheres are linked to functional motor recovery after stroke (van Meer et al. 2010). The assumption was that a change toward an increase in IHC (PDC) values was associated with the proposed (BCI)

training intervention. Accordingly, a within-group analysis was performed: one-tailed paired-sample t-test ($p<0.05$; FDR-corrected) was performed in each group (BCI and CTRL) to determine whether significant differences (ie, increases in PDC) in each estimated connectivity value (ie, without thresholding) could be detected after the experimental (BCI) and control (MI alone) interventions. Consequently, one adjacent matrix was generated for each intervention group and at each frequency band, and the number of the IHCs that were significantly "reinforced" after training (POST vs PRE) was extracted.

To validate the procedure and eventually determine the significance of the derived IHC values, their empirical distribution in the null case was computed by randomly shuffling the PDC values over the entire connectivity network (thus disrupting the network topology) in the PRE and POST conditions for each patient and across frequencies. Then, the distribution of the null case was obtained, evaluating the significant POST-PRE increase in IHC values of the random matrices, and the number of randomly "reinforced" IHCs was counted. This procedure was reiterated (up to 1000 times), and the significance threshold at the 95th percentile was computed for each experimental group.

2.2.4.2 Results

Results of the within-group analyses are shown in Figure 2.1: IHC patterns varied after training as a function of the oscillatory frequency bands in the BCI and CTRL groups. As illustrated in Figure 2.1, the extracted number of reinforced IHCs after training (ie, the number of connections with post-training PDC values that rose significantly by 1-tailed paired-sample t test) exceeded that estimated for the null hypothesis network in the beta1 and beta2 frequency bands (30 and 35, respectively) for the BCI group, whereas this pattern occurred in theta and alpha bands for the CTRL group (29 and 26, respectively).

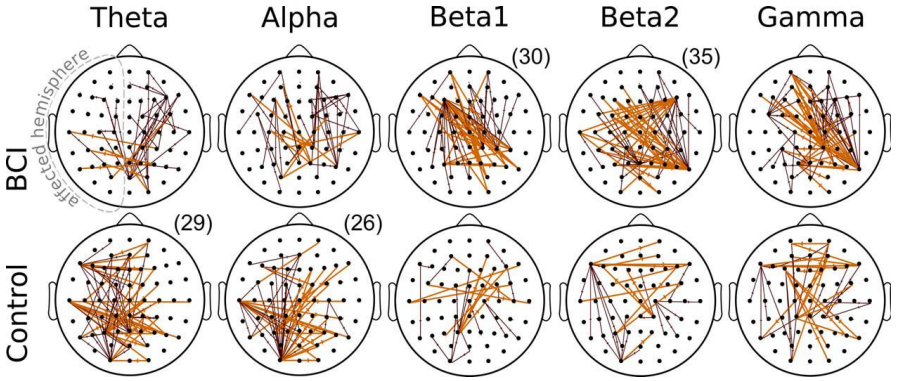

Figure 2.1. Statistical connectivity patterns estimated for the BCI (upper row) and CTRL groups (lower row) in the resting state. The PRE and POST conditions were contrasted to highlight significantly stronger connections in the POST session (1-tailed paired-sample t test, $p < 0.05$, FDR corrected). The scalp model is seen from above, with the nose pointing toward the upper part of the page, and affected hemisphere is shown on the left side of the scalp. Connections between electrodes are represented by lines (orange for interhemispheric connections [IHCs], burgundy for others). The number of significantly reinforced IHCs is reported in parentheses when above the null case.

2.3 Development of a statistical approach for the single subject assessment

2.3.1 Simulation Study 1: Evaluation of the effects of Inter-Trials Variability on PDC accuracy

During an experimental session characterized by a certain number of repetitions, the stationarity of the data across the trials cannot be easily guaranteed, due to many possible reasons (different signal-to-noise ratio; subjects' fatigue or lack of concentration; oscillations in the task performances, especially in the case of pathological subjects). Such inter-trials variations may result in a pattern with a modified density (absence of some connections or presence of spurious links) or variability in the values of existing connections. To take account of these two different phenomena, we considered separately the effects of density changes and the effects of connections value variations.

The simulation study involved the following steps (Figure 2.2):

1. Definition of a connectivity model *A* composed by 10 nodes (brain regions) with a density equal to 30% of all possible connections. Connections weights a_{ij} (i,j = 1,…,10) were selected in the range [0.1÷ 0.9].
2. Generation of different simulated EEG datasets characterized by 100 trials each: a percentage of these trials were generated considering a modified version of the model (factor *Modified Trials*: 1%, 10%, 30%, 50%). For the analysis of density variations effects, the modified models were generated subtracting some connections or adding spurious links with values belonging to the range of the existing connections (factor *N*: -10%, 10%, 20%, 30%; these percentages are calculated on the number of connections existing in the model *A*), while for the investigation of the effects of the links value variability, we considered the following factors:
   i. *Connections Number*, number of connections with a variation in their value (level: 10%, 20%, 50%);
   ii. *Connections Value*, percentage of variation (both increases and decreases with respect to the correct weight) in the connections value (level: 1%, 20%, 50%, 70%).

   For the EEG data generation, the initial time series ($x_1(t)$) is a real signal acquired at the scalp level during a high resolution EEG recording session from a healthy subject in open-eyes rest condition. For each level of factor *Modified Trials*, the other signals $x_2(t),\ldots, x_{10}(t)$ were iteratively achieved according to the predefined scheme: for example for Modified Trials = 30%, the 70% of trials were generate considering the original model (defined at step 1) and the other 30% were generated starting

from its modified version. For each trial, the signal $x_j(t)$ is obtained adding uncorrelated Gaussian white noise (SNR = 3) to all the contributions of other signals $x_i(t)$ (with $i \neq j$), each of which amplified of a_{ij} and delayed of τ_{ij} (the delay values were selected in the range [1÷2]).

3. Estimations, for each of the 100 dataset, of MVAR coefficients (model order equal to 16) and PDC. The significance of estimated connectivity patterns was assessed by the asymptotic statistic procedure.
4. Computation of the performance indices. As for the effects of density changes, we evaluated the total percentage of false positives with respect to the predefined model, while for the investigation of variability in the connections value we defined a *Connections Value Error e* as in the following:

$$e = \frac{1}{N_c} \sum_{k=1}^{N_c} \frac{|a_{ij}^* - a_{ij}|}{a_{ij}} \qquad (2.6)$$

where N_c is the number of connection existing in the model A (defined at step 1), a_{ij} is the value of connection from signal j to signal i in the model A and a_{ij}^* is the estimate of the same connection ($j \rightarrow i$) obtained with the EEG dataset generated for a specific combination of factor under investigation.

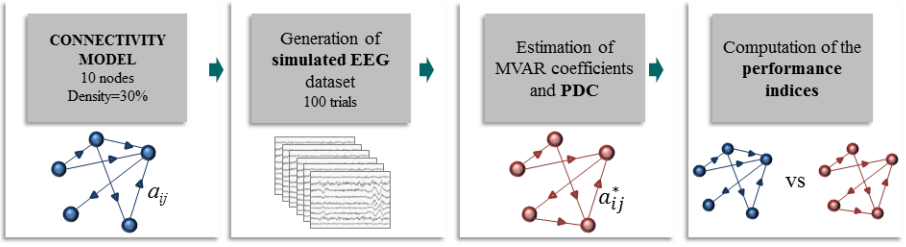

Figure 2.2. Steps sequence of simulation study 1.

To improve the robustness of the statistical analysis, the generation of dataset under each combination of factors was repeated 100 times.

Analysis Of Variance (ANOVA) for repeated measures of the percentage of false positives was performed to evaluate the effects of factors *Modified Trials* and *N* (number of subtracted/added connections). For the study of the effects of connections value variability, ANOVA was performed with *Connections Value Error* as dependent variable and considering the factors*: Modified Trials*, *Connections Number* and *Connections Value*. Duncan's post-hoc tests were applied to further investigate statistical differences in the levels of ANOVAs within factors.

2.3.2 Results

Figure 2.3 shows the results of ANOVA performed to investigate the effects of density variations with the number of false positives as dependent variable. For this analysis two factors were considered: *Modified Trials* (level: 1%, 10%, 30%, 50%) and number *N* of subtracted/added links (level: -10%, 10%, 20%, 30%). Results demonstrate that the number of false positives increases significantly both with the number of modified trials and with the presence of spurious links. In particular, in the investigated ranges of the factors, the percentage of false positives remains below 2% when 10% of connections were removed or added regardless the amount of modified trials. In the case of 20% of added connections, the number of false positives is just over the 5% only when the EEG dataset is characterized by only an half of uniform trials. Lastly, the case of 30% of added connections shows a steeper trend, reaching the 10% of false positives in the estimation.

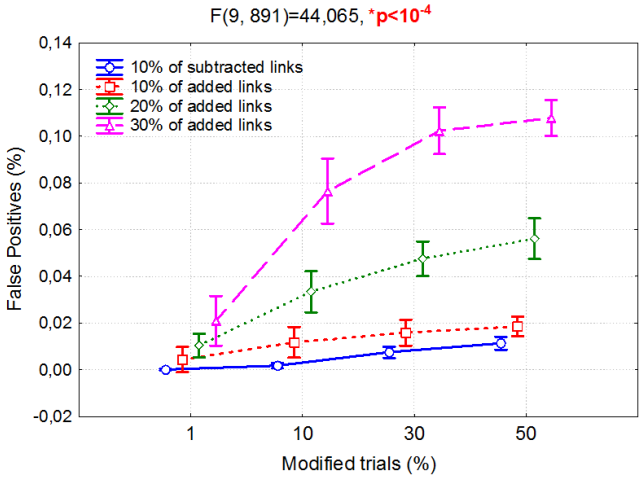

Figure 2.3. ANOVA performed on the number of false positives: plot of means with respect to the factor *Modified Trials* and *N* (percentage of subtracted/added links).

In Figure 2.4, the results of ANOVA performed to investigate the effects of the variability of links value are shown. In this analysis, the performance parameter is a measure of the accuracy in the estimate of the connections values. Three factors were considered: *Modified Trials* (level: 1%, 10%, 30%, 50%), *Connections Number* (level: 10%, 20%, 50%) and *Connections Value* (level: 10%, 20%, 50%, 70%). Results demonstrate that all the factors are significant. In figure 2.4a, the error shows an increasing trend with the number of modified trials, while in figure 2.4b the effect of the other two factors is shown: in this case only when a greater connections number is changed, the amount of variation imposed to the value significantly increases the error.

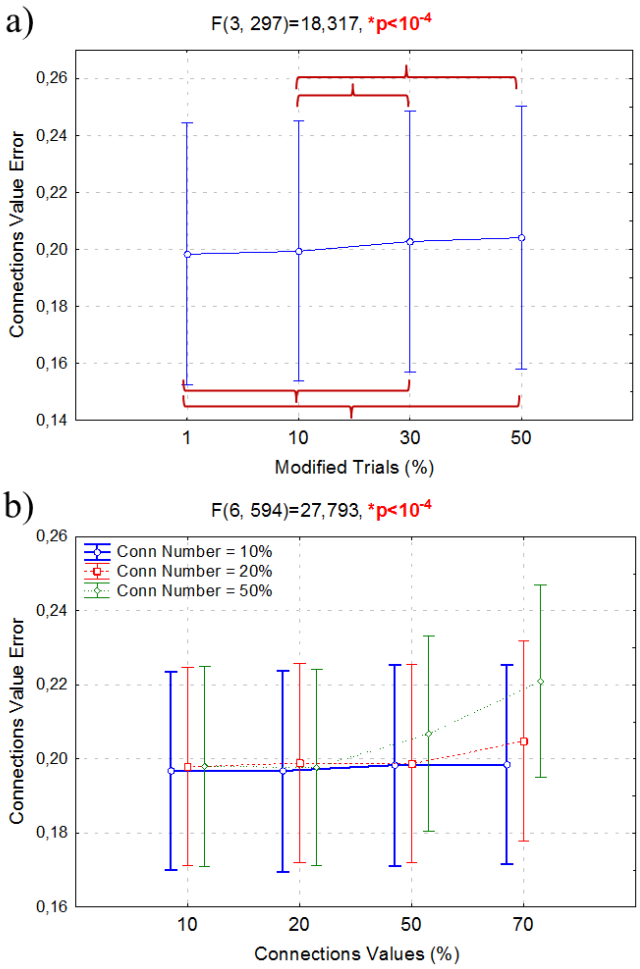

Figure 2.4. ANOVA performed on the Connections Value Error. a) plot of means with respect to the factor *Modified Trials*; b) plot of means with respect to the factor *Connection Number* (number of connections on which to apply a value variation) and *Connections Value* (percentage of variation in the value of existing connections).

2.3.3 Resampling approaches

To achieve a distribution of connectivity estimations during a multi-trial experimental condition, in this study we exploited two approaches, both based on the resampling of an EEG dataset characterized by a certain number of trials N_T: the Jackknife (Tukey 1958) and the bootstrap (Efron

1979). Both approaches can be applied for a number *K* of replications, allowing to obtain *K* EEG dataset to be subjected to the connectivity estimation.

Jackknife consists of a leave-*N*-out approach to trials, where *N* is the percentage of trials to be randomly excluded from the estimation at each replication *K*: as a consequence, the *k*th (*k=1,…,K*) replication of the dataset is characterized by a number of trials N_E which is reduced with respect to the whole initial dataset:

$$N_E = N_T - \frac{N_T \times N}{100} < N_T \tag{2.7}$$

The bootstrap is based on a different approach, consisting of keeping constant the number of trials through the exclusion of some of them and the repetition of others, as shown in equation 2.8:

$$N_E = N_T - \frac{N_T \times N}{100} + r \times t = N_T \tag{2.8}$$

where N_E is the number of trials of each *k* (*k=1,…,K*) replication of the dataset, *N* is the percentage of trials to be randomly excluded and *t* is the number of trials to be repeated *r* times (*r* and *t* are not independent, as their product must be equal to $\frac{N_T * N}{100}$).

2.3.4 Simulation Study 2: Evaluation of the properties of the connectivity distribution obtained applying a resampling approach to EEG dataset

In order to test the distribution of connectivity patterns obtained by the proposed approach, a simulation study was performed (Figure 2.5). Starting from a set of EEG data, obtained from a resting-state recording in a healthy subject, both approaches were applied systematically varying the following factors:

- number of iterations of the resampling procedure (factor *K*; three levels: 50, 500, 5000);
- percentage of excluded trials in the Jackknife procedure (factor *N;* three levels: 2%, 10%, 50%);
- percentage of excluded trials (factor *N;* 3 levels: 2%, 10%, 50%) and number of repetitions of the *t* trials (factor *r;* 3 levels: 1, 2, 4) in the bootstrap procedure.

To evaluate the effect of such factors on the variability of the obtained connectivity distribution, we computed two performance parameters as described as follows.

The Frobenius norm of standard deviation, along the resampling iterations, of connectivity estimation. In equation 2.9, the formulation of Frobenius norm of the N_n x N_n matrix SD of standard deviation (N_n is the number of channels) is shown:

$$\|SD\|_F = \left(\sum_{i=1}^{N_n} \sum_{j=1}^{N_n} sd_{ij}^2 \right)^{1/2} \tag{2.9}$$

where sd_{ij} is the entry ij of matrix SD.

A second measure was computed to evaluate the distribution properties, the Mean Percentage Bias (MPB) defined as follows:

$$MPB = \frac{\sum_{i,j=1}^{N_n} \left(\frac{|a_{ij}^R - a_{ij}|}{a_{ij}} * 100 \right)}{N_n(N_n - 1)} \tag{2.10}$$

where

- a_{ij}: the entry ij of connectivity estimate obtained considering all trials;

- a_{ij}^{R}: the entry ij of connectivity estimate obtained with the resampling approach
- N_n: number of signals.

Figure 2.5. Steps sequence of simulation study 2.

These dependent variables were subjected to two ANOVAs for repeated measures, with 2 within factors (*K*, *N*) and 3 within factors (*K*, *N*, *r*) for Jackknife and Bootstrap, respectively.

2.3.5 Results

Results of the ANOVAs performed on the norm of standard deviation revealed that the choice of the factor *K* (resampling iterations number), in the proposed range, has no significant effect on any of the methods, whereas the parameters *N* and *r* associated to the two approaches significantly influence the variability of the distributions. Fig. 2.6a shows how the standard deviation increases significantly with the number of excluded trials (*N*) in Jackknife approach. The norm of standard deviation range is ($5x10^{-2} \div 2x10^{-1}$). Similarly, in the case of bootstrap (Fig. 2.6b) the norm significantly increases with parameter *N* but also with parameter *r*. In this case, standard deviation range is a little bit wider ($5x10^{-2} \div 3{,}1x10^{-1}$). The same trend was obtained for the Mean Percentage Bias parameter (Fig. 2.6c for Jackknife, Fig. 2.6d for Bootstrap): in all the conditions, MPB values are of the magnitude order of 10^{-2}, revealing the stability of PDC estimator.

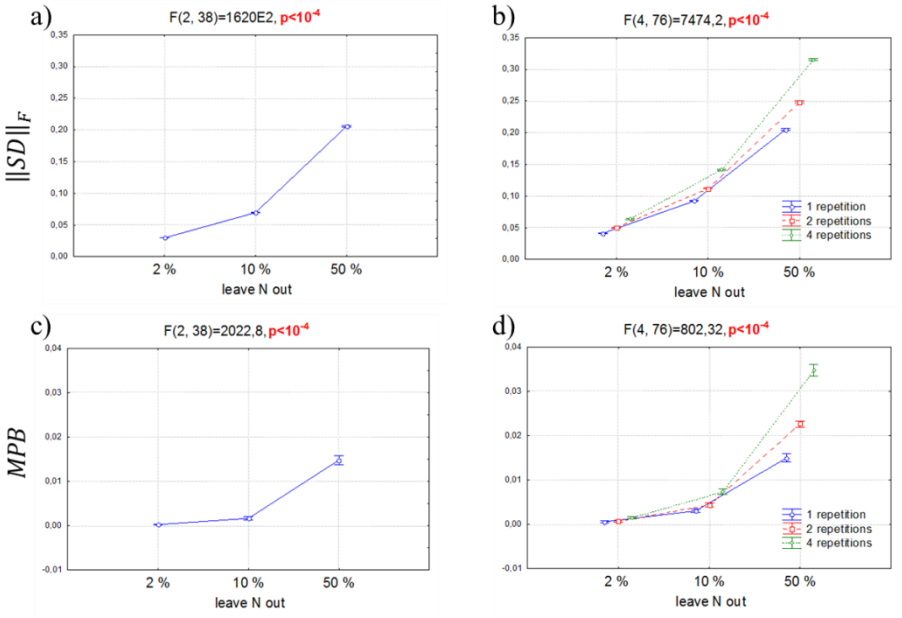

Figure 2.6. ANOVAs performed on performance parameters. Plots of means of the norm of standard deviation ($\|SD\|_F$) of the connectivity distribution (panel a) and of the Mean Percentage Bias parameter (panel c) with respect to the factor *N* (number of trials excluded) for Jackknife approach; plots of means of $\|SD\|_F$ (panel a) and of the MPB parameter (panel d) with respect to the factors *N* (number of trials excluded) and *r* (number of repetitions of *t* trials) for Bootstrap approach.

2.3.6 Simulation Study 3: Evaluation of the performances of the statistical procedure developed for assessing changes in brain connectivity at the single subject level

The steps of the simulation study are detailed as follows:

1. Definition of two pre-imposed connectivity patterns representing two conditions to be compared. Each pattern is represented by a directed, weighted graph. Each condition is characterized by the same structure (same number of nodes, *N=6*; same unweighted adjacency matrix and same delays, according to the scheme in Fig. 2.7), but with different values imposed to some connections (see Fig. 2.7; red links: connections with the same value in the two patterns; green links: connections with different values minimum difference

equal to 0.1). All the values are randomly assigned in the range [0.1:0.9].

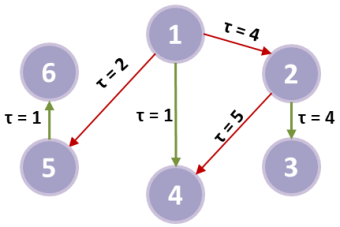

Figure 2.7. Structure of the two connectivity patterns used in the simulation study to reproduce two different conditions: red links indicate connections with same value in the two patterns, while green links indicate connections with different values (minimum difference: 0.1).

2. Generation of simulated EEG datasets characterized by N_T trials, fitting the two predefined patterns. For the EEG data generation, the initial time series ($x_1(t)$, signal from node 1) is a real potential acquired at the scalp level during a high resolution EEG recording session from a healthy subject in open-eyes rest condition. The other signals $x_2(t),\ldots,\ x_6(t)$ were iteratively achieved according to the predefined scheme: the signal $x_j(t)$ (j=2,…,6) is obtained adding uncorrelated Gaussian white noise (SNR = 1) to all the contributions of other signals $x_i(t)$ (with $i \neq j$), each amplified of a_{ij} and delayed of τ_{ij}.

3. This procedure was repeated for different levels of factor Trials Number (4 levels: 10, 50, 100, 200) selected in order to model different practical experimental condition, ranging from a limited availability of data (10 trials) to a great data amount (200 trials).

4. For the 3 levels of factor Trials Number (50, 100, 200) the resampling approaches were applied, systematically varying the following factors:

- number of replications of the resampling procedure (factor *K*; two levels: 20, 200);
- percentage of trials excluded in the Jackknife procedure (factor *N*; three levels: 10%, 20%, 50%);
- percentage of trials excluded (factor *N*; three levels: 10%, 20%, 50%) and number *r* of repetitions of the *t* trials, with $t = (N_T \times N)/(r \times 100)$ (factor repetitions; three levels: 1, 2, 4) in the bootstrap procedure.

5. As not all combinations of previous factors could be performed with level Trials Number=10, due to the limited amount of data, to consider in the same analysis all the levels of factor Trials Number (10, 50, 100, 200), the resampling approaches were also applied considering the following subgroups of factors:
   - Jackknife: Replications (1 level *K=20*), percentage of excluded trials *N* (2 levels: 20%, 50%);
   - Bootstrap: Replications *K* (2 levels: 20, 200), percentage of excluded trials *N* (levels: 20%, 50%), repetitions *r* (2 levels: 1, 2).
6. PDC estimation was performed for each dataset *k*, obtaining the two connectivity distributions related to the two patterns defined at step 1.
7. Statistical comparison between the two distributions for each connections (significance level of 0.05, FDR correction) was performed. We compared two kinds of approaches:
   - parametric method: independent two-sample t-test;

- nonparametric method: we compared the estimated conditions in one condition (second pattern) with the distribution related to the other condition (first pattern). If the values in the second pattern were above (below) the thresholds related to the percentiles of 97.5% (2.5%) of the distribution of the first pattern we took them as significantly reinforced (weakened) with respect to the first condition.

8. Extraction of indices of performance. We evaluated two indices:

   - Accuracy in the evaluation of connections with same value (the higher the accuracy, the lower the rate of false positives);

   - Accuracy in the evaluation of differences (the higher the accuracy, the lower the rate of false negatives);

   Both measures are defined as follow:

$$A = \frac{1}{N_F}\sum_{i=1}^{N_F} A_{F\,i} = \frac{1}{N_F}\sum_{i=1}^{N_F}\left(\frac{1}{N_C}\sum_{n=1}^{N_C} h_n\right) \qquad (2.11)$$

   where N_F is the number of frequencies (N_F = 45 considering the typical range of EEG signals [1:45] Hz), A_{Fi} the accuracy obtained at the frequency i, N_C is the number of connections of interest (N_C =3 both considering connections with same values and connections with different values) and h_n is a logical variable equal to 1 when the statistical test provide a correct answer in the evaluation of connection n (i.e. satisfied null hypothesis considering connections with same values, while revealed statistical differences considering connections with different values), otherwise h_n=0.

9. All the previous steps were repeated 100 times for each combination of factors, and, separately for each resampling method. The obtained

results were subjected to repeated measures ANOVAs, computed considering as dependent variables the indices of performance. In particular separate ANOVAs were performed for the step 4 and 5 considering the appropriate within factors for each case.

2.3.7 Results

2.3.7.1 Jackknife performances

For the Jackknife, results of the ANOVAs performed on the accuracies in the detection of statistical differences, are reported in Table I: in particular, for the accuracy related to the connections with same values, the factors replication, *N*, Statistical Test are significant, while for the connections with different values all the factors influence significantly the accuracy except for Statistical Test.

TABLE I

RESULTS OF THE ANOVAS COMPUTED CONSIDERING AS DEPENDENT VARIABLES THE PERFORMANCE PARAMETERS FOR THE JACKKNIFE APPROACH

	Connections with same value		Connections with different value	
	F	p	F	p
Statistical test (*ST*)	**$5.2 * 10^4$**	**$<10^{-4}$**	0.194	0.661
Replication (*K*)	**6.55**	**0.012**	**13.0**	**$<10^{-4}$**
Trials Number (*T*)	**0.006**	**0.994**	**46.02**	**$<10^{-4}$**
leave N out (*N*)	**3269.5**	**$<10^{-4}$**	**66.76**	**$<10^{-4}$**
*ST * K*	**4715.1**	**$<10^{-4}$**	**86.25**	**$<10^{-4}$**
*ST * T*	0.902	0.407	1.796	0.169
*K * T*	0.996	0.371	0.857	0.426
*ST * N*	**1422.5**	**$<10^{-4}$**	0.033	0.968
*K * N*	**53.4**	**$<10^{-4}$**	3.952	0.021
*T * N*	0.643	0.632	**8.653**	**$<10^{-4}$**
*ST * K * T*	0.763	0.468	**10.02**	**$<10^{-4}$**
*ST * K * N*	**159.7**	**$<10^{-4}$**	**28.27**	**$<10^{-4}$**
*ST * T * N*	1.502	0.201	2.38	0.051
K T * N*	1.248	0.290	0.70	0.594
*ST * K * T * N*	0.751	0.558	**4.412**	**0.002**

2.3.7.2 Effect of the variability introduced in the distribution

In Figure 2.8 the results of the interaction between factors K (Replications), N (number of removed trials) and ST (Statistical Test) are shown: panels a) and b) are related to the connections with same values and with different values, respectively. The obtained trends for the connections with same value showed that the accuracy increases with the percentage of excluded trials and with the number of replications; furthermore, comparisons performed with t-test show a higher number of false positives

with respect to the nonparametric test. Instead, for the connections with different values, the accuracy decreases with the percentage of excluded trials and with the number of replications and increases with trials number. In this case the variability range of the performance index is smaller than the previous case and the accuracy is always higher than 95%. By choosing a combination of factors it is possible to obtain a trade-off between the two effects (Fig.2.8: 92% in the evaluation of connection with same value and 95% for the statistical differences using leave 50% out – 200 Replications – non parametric test).

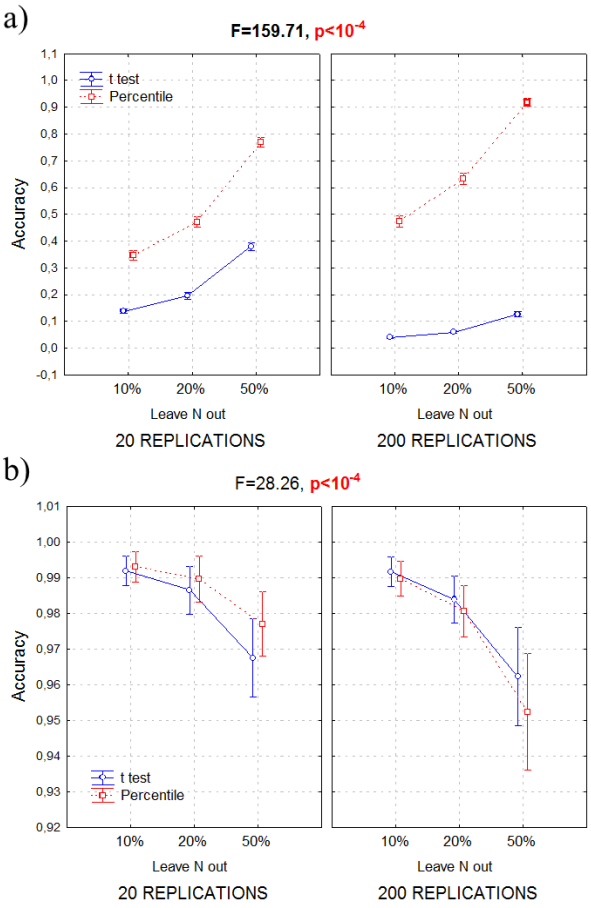

Figure 2.8. Results of ANOVA performed considering as dependent variables the performance parameters obtained with Jackknife method: panels a) and b) show the results related to the connections with same values and with different values, respectively; plot of means of the interaction between all the factors characterizing Jackknife (Replication-*N*-Statistical Test-Trials). The bar on each point represents the 95% confidence intervals of the mean errors.

2.3.7.3 Effects of the amount of data

To study also the case in which an EEG dataset is characterised by few repetitions, we performed for the Jackknife a separate ANOVA with 4 levels of factor Trials Number (10, 50, 100, 200) and selecting subsets of levels for the factors Replications (*K=20*) and percentage of excluded trials *N* (levels:

20%, 50%) due to the limited number of combinations that can be performed with only 10 items. In Figure 2.9 the results related to the interaction between factors *N*-Statistical Test-Trials are shown. From these results, in the case of few trials the statistical comparison between two connectivity patterns distributions returns lower levels of accuracy for the links with different values, while no significant effect resulted for the links with the same value. Focusing on the 10 trials condition, with a proper choice of parameters (leave 50% out, nonparametric test), the accuracy is good (around 80%) both in the cases of connections with same values and different values.

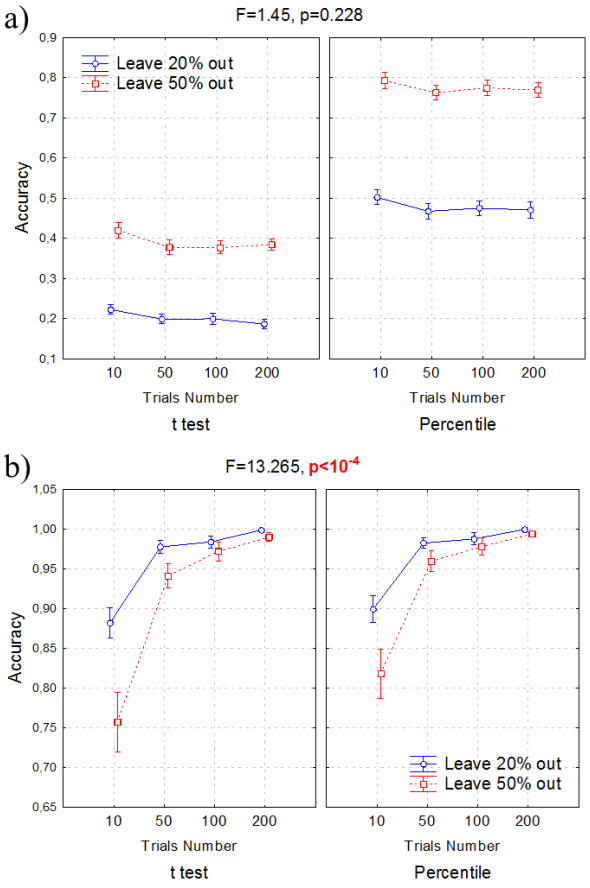

Figure 2.9. Results of ANOVA performed considering as dependent variables the performance parameters obtained with Jackknife method: panels a) and b) report the results related to the connections with same values and with different values respectively, both related to the level *K*= 20 replications; plot of means of the interaction between factors *N*-Statistical Test-Trials considering also the level Trial Number = 10. The bar on each point represents the 95% confidence intervals of the mean errors.

In summary, results show that, as expected, the accuracy related to false positives and to false negatives are affected by the variability introduced in the data in an opposite way (higher N, higher accuracy in correctly detecting connections with the same value and lower accuracy in detecting connections with different values). However, an appropriate selection of

different parameters can provide a trade-off between the two effects and allows to reach a high level of accuracy.

2.3.7.4 Bootstrap performances

For the bootstrap, the results of the ANOVAs are reported in table II (only a sub-set of the most interesting interactions between factors is shown): in this case all the main factors are significant for both accuracy indexes.

TABLE II

RESULTS OF THE ANOVAS COMPUTED CONSIDERING AS DEPENDENT VARIABLES THE PERFORMANCE PARAMETERS FOR THE BOOTSTRAP METHOD

	Connections with same value		Connections with different value	
	F	p	F	p
Statistical test (*ST*)	**$2.3 * 10^5$**	**$<10^{-4}$**	**110.4**	**$<10^{-4}$**
Replication (*K*)	**250.9**	**$<10^{-4}$**	**42.12**	**$<10^{-4}$**
Trials Number (*T*)	**10.9**	**$<10^{-4}$**	**179.31**	**$<10^{-4}$**
leave N out (*N*)	**6132.7**	**$<10^{-4}$**	**214.62**	**$<10^{-4}$**
repetition (r)	**1149.7**	**$<10^{-4}$**	**40.95**	**$<10^{-4}$**
*ST * K*	**$3.7 * 10^4$**	**$<10^{-4}$**	**1505.4**	**$<10^{-4}$**
*ST * T*	**8.282**	**$<10^{-3}$**	0.915	0.402
*K * T*	0.956	0.386	1.766	0.174
*ST * N*	**1298.3**	**$<10^{-4}$**	0.123	0.884
*K * N*	**324,7**	**$<10^{-4}$**	0.919	0.401
*T * N*	**3.718**	**0.006**	**17.104**	**$<10^{-4}$**
*N * r*	**3.09**	**0.016**	**6.402**	**$<10^{-4}$**
*ST * K * T*	1.818	0.165	**30.5**	**$<10^{-4}$**
*ST * N * r*	**89.04**	**$<10^{-4}$**	0.622	0.647
*ST * K * N * r*	**9.18**	**$<10^{-4}$**	1.088	0.362
*ST * K * T * N*	0.628	0.643	**3.105**	**0.016**

2.3.7.5 Effect of the variability introduced in the distribution

As shown by Fig. 2.10, the trends obtained with the Bootstrap are similar to those obtained by the Jackknife procedure (Fig. 2.8):

- in the case of connections with same values, the accuracy increases with the percentage of excluded trials (*N*), with the number of Replication and with the number of repetitions *r* of some trials; t-test shows a higher number of false positives with respect to the nonparametric test.
- for the connections with different values, the accuracy decreases with the percentage of excluded trials *N*, with the number of Replications and with the number of repetitions *r* of some trials.

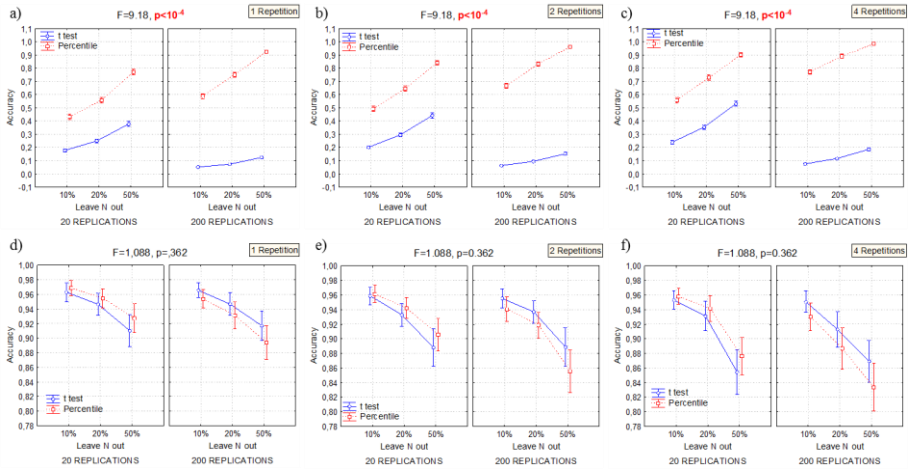

Figure 2.10. Results of ANOVA performed considering as dependent variables the performance parameters obtained with Bootstrap method: panels a), b), c) report the results related to the connections with same values for *r*=1, *r*=2, *r*=4 respectively; panels d), e), f) report the results related to the connections with different values for *r*=1, *r*=2, *r*=4 respectively; plot of means of the interaction between factors Replication-*N*-Statistical Test-repetition. The bar on each point represents the 95% confidence interval of the mean errors.

Also for Bootstrap it is possible to select a combination of choices to maximize the accuracy both in the correct detection of links that are kept

constant across conditions and of those which change. However, the maximum level of accuracy that can be achieved is lower with respect to the Jackknife. By selecting N=50%, r=1, K=200, both accuracies are around 90% (Fig.2.10a and 2.10d): variations in this choice lead to an increase of the false positives or of the false negatives.

2.3.7.6 Effects of the amount of data

Figure 2.11 shows the results of the second ANOVA performed for Bootstrap for considering also the level Trials Number=10 (interaction between factors: Replication-*N*-Statistical Test-Trials). As the bootstrap maintains constant the number of trials, the subsets investigated for the other factors are characterised by a greater number of levels with respect to the Jackknife:

- Replications *K* (levels: 20, 200)*;*
- Trials number *T* (levels: 10, 50, 100, 200)*;*
- percentage of excluded trials *N* (levels: 20%, 50%);
- repetitions *r* (levels: 1, 2).

Also here, the trends are similar to those of Jackknife. In particular, in the case of 10 trials a set of parameters for a trade-off between the accuracy in false positives and false negatives could be:

- 200 replications, leave 50% out, nonparametric test: high accuracy in the evaluation of connections with same values (90%), but higher probability of committing false negatives with respect to the Jackknife (accuracy of 60%);
- 200 replications, leave 20% out, nonparametric test: 70% of accuracy in the case of connections with same values and 80% in the evaluation of connections with different values.

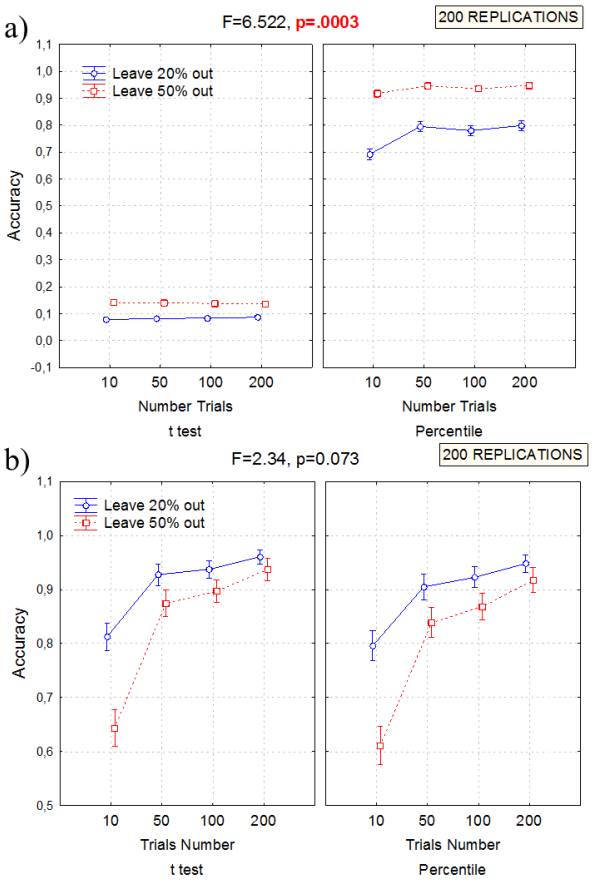

Figure 2.11. Results of ANOVA performed considering as dependent variables the performance parameters obtained with Bootstrap method: panels a) and b) report the results related to the connections with same values and with different values respectively, both related to the level *r*= 1 repetition; plot of means of the interaction between factors *Replication-N-StatTest-Trials* considering also the level Trial Number = 10. The bar on each point represents the 95% confidence interval of the mean errors.

2.3.8 Application to real EEG data: motor task

2.3.8.1 Experimental design

Based on the results of simulation study, the procedure characterized by highest level of accuracies was tested on EEG data acquired from 12 subacute stroke patients (mean age, 62.1 ± 9.9 years; time since event, 1.75 ±

1.2 month; unilateral lesion, 6 left/6 right affected hemisphere) enrolled from the rehabilitation hospital ward at Fondazione Santa Lucia, Rome, Italy. All these patients underwent standard motor rehabilitation for the upper limb and an add-on newly proposed intervention based on a BCI-assisted upper limb motor imagery training (Pichiorri et al. 2015), as described in the previous section. Immediately before and after the training intervention, the patients were subjected to two screening sessions (PRE and POST sessions) including clinical assessment and high density EEG recordings at rest and during the attempt of a simple movement by the hand affected by the motor deficit.

In each screening session, the patient was comfortably seated in an armchair placed in a dimly lit room with his/her upper limbs on a desk, visible to him/her, with hand posture on a side view and he/she was asked to start perform the motor task (attempted grasping movement by the affected hand) respecting the trials timeline described in the previous section (see Fig. 1.1).

2.3.8.2 Signal processing

Data preprocessing included down-sampling at 100 Hz, band pass filtering (1÷45 Hz) and artifact rejection (Independent Component Analysis to remove ocular artifacts and threshold criteria (±80 μV) for residual artifacts). For the connectivity analysis, we selected the 4 s of each trial related to the attempted movement phase, which were further divided in 1s-epochs to reduce the amount of trials rejected to avoid artifacts. This procedure returned (for each patient and each condition) an EEG dataset consisting of approximately 60 artifact-free trials.

According to the results of the simulation study, we applied the Jackknife approach, setting parameters as follows:

- Replications $K = 200$;
- percentage of excluded trials $N = 50\%$.

Brain connectivity was estimated from 29 channels (Fp1, Fpz, Fp2, F7, F3, Fz, F4, F8, FC5, FC1, FC2, FC6, T7, C3, Cz, C4, T8, CP5, CP1, CP2, CP6, P7, P3, Pz, P4, P8, O1, Oz, O2). This subset of signals was selected to ensure the robustness of the estimator, also because, for scalp analysis, the spatial sampling above 30 electrodes is redundant, due to the correlation between neighboring electrodes. The connectivity patterns achieved for each frequency in the range [1:45] Hz were averaged within 5 frequency bands, defined for each patient according to Individual Alpha Frequency (Klimesch 1999): theta [IAF-6;IAF-2], alpha [IAF-2;IAF+2], beta1 [IAF+2;IAF+11], beta2 [IAF-11;IAF+20] and gamma [IAF+20;IAF+35].

Once the patterns distributions were obtained for each patient, condition and frequency band, we performed the statistical comparison between PRE and POST conditions by means of the percentile approach, which had returned the best performances in the simulation study.

To evaluate the effects of the rehabilitative intervention, we focused on the pattern that was significantly reinforced for each patient in the POST with respect to the PRE session.

2.3.8.3 Results

The application of the described procedure to the stroke patients EEG data allowed to obtain for each subject the connectivity pattern reinforced at the end of the rehabilitative training. Figure 2.12 shows the network obtained for a patient with left affected hemisphere: the pattern in the motor-related frequency band (beta1) shows a higher involvement of channels over the motor areas of the left hemisphere during the attempt to move the right hand.

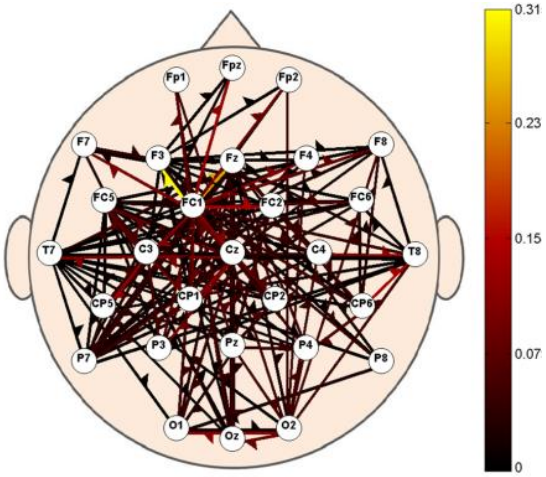

Figure 2.12. Reinforced connectivity pattern obtained in beta1 band (typical of sensory-motor rhythms) for a representative patient with lesion in the left hemisphere. The scalp is seen from the above, with the nose pointing to the upper part of the page. Effective connections between the brain regions are represented by arrows whose color and diameter code for the corresponding connectivity values estimated by means of PDC.

2.4 Discussion

2.4.1 Methodological considerations

The present section addressed some open issue related to the estimation and validation of effective connectivity starting from EEG signals. In particular, after the description of the state of the art methods , three simulation study were designed to reach the following specific aims:

- evaluation of the effects of Inter-Trials Variability (ITV) on PDC accuracy;
- evaluation of the properties of the connectivity distribution that can be built applying a resampling approach to EEG dataset:

- evaluation of the performances of the proposed statistical procedure based on resampling approach for assessing changes in brain connectivity at the single subject level.

The first simulation study was performed with the aim to evaluate the accuracy and robustness of PDC estimator on EEG data characterized by different levels of inter-trials variability. EEG datasets were generated imposing modified versions of a predefined model on a certain number of trials. The results of this study demonstrate the robustness and the accuracy of the PDC under a large range of conditions usually encountered in practice. In particular, the effects of density variations showed that the false positives exceed the 5% only when the density in strongly increased in a considerable number of trials. The study on the effect of variations in the connections value demonstrated that for a high number of modified connections, the variations imposed on the value are related to a significant increase of the error. Thus the robustness and the accuracy of PDC patterns were reinforced simulating conditions that can be encountered in practice.

The two methods here evaluated for resampling the EEG data have proved to be able to produce a distribution of connectivity in a single condition and for a single subject, allowing statistical analysis (Simulation Study 2). As might be expected, the standard deviation of such distribution increases with the number of excluded trials, for both approaches. The mean Percentage Bias index showed the same increasing trend, but the values obtained in all conditions are related to high accuracy of the connectivity estimator.

At last, the third study addressed the systematic evaluation of the performances of the two resampling approaches when applied to multi-trial EEG data with the purpose to build a distribution of connectivity in a specific condition and to compare different conditions for a single subject.

The performances of Bootstrap and Jackknife approaches have been investigated under different choices of their own characterizing parameters and for different levels of data amount.

Four aspects have been investigated through the simulation study:

i) the selection of parameters characterizing the resampling methods (number *N* of trials left out for Jackknife, the same number *N* plus the number *r* of repetitions of the same trials for bootstrap);

ii) the effect of a reduced/extended amount of data for the procedure (i.e. number of trials available for the resampling);

iii) the procedure for the statistical comparison between connectivity distributions;

iv) the comparison between the two approaches.

Regarding the first point, the results of simulation study showed that a higher level of variability introduced in the EEG dataset distribution (e.g. 50% of excluded trials for Jackknife, *N*=50% and *r*=4 for Bootstrap) affects the detection of similarities and differences in an opposite way (higher rate of false positives and lower rate of false negatives). This result was expected, and can be addressed by choices that allow a trade-off between the two effects, by keeping the maximum accuracy on both aspects. The simulation results can provide useful information in this respect, showing which factors affect more the performances and suggesting a procedure that allows to achieve the best overall performances (Fig. 2.8 and Fig. 2.10).

The second point addresses the influence of the amount of available data on the performances of the proposed procedures. Results obtained for different number of trials (Fig. 2.9 and Fig. 2.11) showed the deterioration of the performances that goes with a reduction of the number of trials, but also how a proper selection of the resampling method and of the statistical test

can however keep both the accuracies around 80 % even in the worst case (10 trials).

As for the kind of statistical test more appropriate for the statistical comparison, the percentile approach provided a good compromise between the correct detection of similarities and differences between the networks. In fact, it showed far better performances in avoiding false positives with respect to the t-test (Fig. 2.8a and 2.9a for the Jackknife and Fig. 2.10a and 2.11a for the bootstrap) and comparable ones in the case of false negatives (Fig. 2.8b and 2.9b for the Jackknife and Fig. 2.10b and 1.11b for the bootstrap).

As for the comparison between the two approaches, they showed general similar trends, but different levels of accuracy. For both procedures, our simulations returned that an appropriate combination of factors can provide overall better performances and a tradeoff between different effects, but the level of accuracy that can be achieved is higher for the Jackknife with respect to the bootstrap, especially when dealing with false positives (cfr. Fig 2.8 with Fig. 2.10 and Fig. 2.19 with Fig.2.11). In previous studies (Petti et al. 2014), (Shao and Tu 2012; Meyer et al. 1986; Efron 1982) the two approaches were compared in terms of characteristic of the obtained distributions (bias, standard error): Efron in (Efron 1982) described the theoretical advantages of the Bootstrap procedure over the Jackknife, while Meyer et al, in a study about the uncertainty in population growth rate (Meyer et al. 1986) concluded that the two techniques produce similar results. Furthermore, the Jackknife requires fewer computations than the Bootstrap, so bootstrapping may not be necessary when the Jackknife can be applied.

A last consideration about the methodological results is related to the different behavior of the procedure in the evaluation of connections with

same values and in the detection of statistical differences. In the latter case, the performances indices are kept in a narrow range, closer to the 100% of accuracy. On the contrary, the procedure of resampling seems to lead often to reject the null hypothesis. This indicates that more attention is needed to avoid incurring in false positives. For this reason, in the application to real data we selected parameters and procedures which showed better performances in such respect.

2.4.2 Application to real EEG data

With respect to the functional neuroimaging techniques described and applied in the previous section, new insights were here provided about the study of plasticity phenomena by means of connectivity estimation.

As first step, the state of the art methods were used to assess the consistent effects of a therapy on the resting state brain networks. For this investigation two within-group analyses were performed (separately for BCI and CTRL groups) and particular attention was focused on the post-training increase in IHC pattern. The obtained results allowed to reveal different behaviors for the two group: indeed IHC patterns varied after training as a function of the oscillatory frequency bands in the BCI and CTRL groups.

Instead, the new statistical procedure proposed in this section was used for the evaluation of the specific effects induced by a rehabilitative training (and so regardless the kind of intervention) at the single patient level. Similarly to the previous group analyses, the attention was focused on the pattern increased as a consequence of the training. For this application motor task attempted with the affected upper limb was studied: brain networks reinforced after the rehabilitation period showed a higher involvement of channels over the motor areas of affected hemisphere.

The next Section will address how an approach based on synthetic descriptors can be useful to capture the more interesting brain networks properties modulated by an intervention.

Section II References

Akaike, H. 1974. “A New Look at Statistical Model Identification.” *IEEE Trans Automat Control* 19: 716–23.

Astolfi, Laura, Febo Cincotti, Donatella Mattia, M G Marciani, Luis A Baccalà, Fabrizio de Vico Fallani, Serenella Salinari, Mauro Ursino, Melissa Zavaglia, and Fabio Babiloni. 2006. “Assessing Cortical Functional Connectivity by Partial Directed Coherence: Simulations and Application to Real Data.” *IEEE Transactions on Bio-Medical Engineering* 53 (9): 1802–12. doi:10.1109/TBME.2006.873692.

Astolfi, Laura, Febo Cincotti, Donatella Mattia, M Grazia Marciani, Luiz A Baccala, Fabrizio de Vico Fallani, Serenella Salinari, et al. 2007. “Comparison of Different Cortical Connectivity Estimators for High-Resolution EEG Recordings.” *Hum Brain Mapp* 28 (2): 143–57. doi:10.1002/hbm.20263.

Baccalá, Luiz A., and Koichi Sameshima. 2001. “Partial Directed Coherence: A New Concept in Neural Structure Determination.” *Biological Cybernetics* 84 (6): 463–74. doi:10.1007/PL00007990.

Blinowska, Katarzyna J. 2011. “Review of the Methods of Determination of Directed Connectivity from Multichannel Data.” *Medical & Biological Engineering & Computing* 49 (5): 521–29. doi:10.1007/s11517-011-0739-x.

Efron, B. 1979. “Bootstrap Methods: Another Look at the Jackknife.” *The Annals of Statistics* 7 (1): 1–26. doi:10.1214/aos/1176344552.

———. 1982. *The Jackknife, the Bootstrap and Other Resampling Plans*. CBMS-NSF Regional Conference Series in Applied Mathematics. Society for Industrial and Applied Mathematics. http://epubs.siam.org/doi/book/10.1137/1.9781611970319.

Friston, K. J., C. D. Frith, and R. S. J. Frackowiak. 1993. “Time-Dependent Changes in Effective Connectivity Measured with PET.” *Human Brain Mapping* 1 (1): 69–79. doi:10.1002/hbm.460010108.

Granger, C. W. J. 1969. “Investigating Causal Relations by Econometric Models and Cross-Spectral Methods.” *Econometrica* 37 (3): 424–38. doi:10.2307/1912791.

Guo, Xiaoli, Zheng Jin, Xinyang Feng, and Shanbao Tong. 2014. “Enhanced Effective Connectivity in Mild Occipital Stroke Patients With Hemianopia.” *IEEE Transactions on Neural Systems and Rehabilitation Engineering* 22 (6): 1210–17. doi:10.1109/TNSRE.2014.2325601.

Horwitz, Barry. 2003. “The Elusive Concept of Brain Connectivity.” *NeuroImage* 19 (2 Pt 1): 466–70.

Kaminski, M. J., and K. J. Blinowska. 1991. “A New Method of the Description of the Information Flow in the Brain Structures.” *Biological Cybernetics* 65 (3): 203–10. doi:10.1007/BF00198091.

Kelly, K.M., D.S. Shiau, R.T. Kern, J.H. Chien, M.C.K. Yang, K.A. Yandora, J.P. Valeriano, J.J. Halford, and J.C. Sackellares. 2010. “Assessment of a Scalp EEG-Based Automated Seizure Detection System.” *Clinical Neurophysiology : Official Journal of the International Federation of Clinical Neurophysiology* 121 (11): 1832–43. doi:10.1016/j.clinph.2010.04.016.

Klimesch, W. 1999. “EEG Alpha and Theta Oscillations Reflect Cognitive and Memory Performance: A Review and Analysis.” *Brain Research. Brain Research Reviews* 29 (2-3): 169–95.

Kuś, Rafal, Maciej Kamiński, and Katarzyna J. Blinowska. 2004. “Determination of EEG Activity Propagation: Pair-Wise versus Multichannel Estimate.” *IEEE Transactions on Bio-Medical Engineering* 51 (9): 1501–10. doi:10.1109/TBME.2004.827929.

Meyer, Joseph S., Christopher G. Ingersoll, Lyman L. McDonald, and Marks S. Boyce. 1986. “Estimating Uncertainty in Population Growth Rates: Jackknife vs. Bootstrap Techniques.” *Ecology* 67 (5): 1156–66. doi:10.2307/1938671.

Murias, Michael, Sara J. Webb, Jessica Greenson, and Geraldine Dawson. 2007. “Resting State Cortical Connectivity Reflected in EEG Coherence in Individuals with Autism.” *Biological Psychiatry* 62 (3): 270–73. doi:10.1016/j.biopsych.2006.11.012.

Petti, M., S. Caschera, A. Anzolin, J. Toppi, F. Pichiorri, F. Babiloni, F. Cincotti, D. Mattia, and L. Astolfi. 2015. “Effect of Inter-Trials Variability on the Estimation of Cortical Connectivity by Partial Directed Coherence.” In *2015 37th Annual International Conference of the IEEE Engineering in Medicine and Biology Society (EMBC)*, 3791–94. doi:10.1109/EMBC.2015.7319219.

Petti, M., F. Pichiorri, J. Toppi, F. Cincotti, S. Salinari, F. Babiloni, D. Mattia, and L. Astolfi. 2014. “Individual Cortical Connectivity Changes after Stroke: A Resampling Approach to Enable Statistical Assessment at Single-Subject Level.” In , 2785–88. IEEE. doi:10.1109/EMBC.2014.6944201.

Pichiorri, Floriana, Giovanni Morone, Manuela Petti, Jlenia Toppi, Iolanda Pisotta, Marco Molinari, Stefano Paolucci, et al. 2015. “Brain-Computer Interface Boosts Motor Imagery Practice during Stroke Recovery: BCI and Motor Imagery.” *Annals of Neurology* 77 (5): 851–65. doi:10.1002/ana.24390.

Rotondi, Fabio, Silvana Franceschetti, Giuliano Avanzini, and Ferruccio Panzica. 2015. “Altered EEG Resting-State Effective Connectivity in Drug-Naïve Childhood Absence Epilepsy.” *Clinical*

Neurophysiology. Accessed November 18. doi:10.1016/j.clinph.2015.09.003.

Sakoğlu, Ünal, Godfrey D. Pearlson, Kent A. Kiehl, Y. Michelle Wang, Andrew M. Michael, and Vince D. Calhoun. 2010. "A Method for Evaluating Dynamic Functional Network Connectivity and Task-Modulation: Application to Schizophrenia." *Magma (New York, N.Y.)* 23 (5-6): 351–66. doi:10.1007/s10334-010-0197-8.

Sameshima, K., and L. A Baccalá. 1999. "Using Partial Directed Coherence to Describe Neuronal Ensemble Interactions." *Journal of Neuroscience Methods* 94 (1): 93–103.

Shao, Jun, and Dongsheng Tu. 2012. *The Jackknife and Bootstrap*. Springer Science & Business Media.

Stephen, Emily P., Kyle Q. Lepage, Uri T. Eden, Peter Brunner, Gerwin Schalk, Jonathan S. Brumberg, Frank H. Guenther, and Mark A. Kramer. 2014. "Assessing Dynamics, Spatial Scale, and Uncertainty in Task-Related Brain Network Analyses." *Frontiers in Computational Neuroscience* 8 (March). doi:10.3389/fncom.2014.00031.

Takahashi, Daniel Yasumasa, Luis A. Baccalà, and Koichi Sameshima. 2007. "Connectivity Inference between Neural Structures via Partial Directed Coherence." *Journal of Applied Statistics* 34 (10): 1259–73. doi:10.1080/02664760701593065.

Toppi, J., A. Anzolin, M. Petti, F. Cincotti, D. Mattia, S. Salinari, F. Babiloni, and L. Astolfi. 2014. "Investigating Statistical Differences in Connectivity Patterns Properties at Single Subject Level: A New Resampling Approach." In *Engineering in Medicine and Biology Society (EMBC), 2014 36th Annual International Conference of the IEEE*, 6357–60. IEEE. http://ieeexplore.ieee.org/xpls/abs_all.jsp?arnumber=6945082.

Toppi, J., F. De Vico Fallani, G. Vecchiato, A. G. Maglione, F. Cincotti, D. Mattia, S. Salinari, F. Babiloni, and L. Astolfi. 2012. "How the Statistical Validation of Functional Connectivity Patterns Can Prevent Erroneous Definition of Small-World Properties of a Brain Connectivity Network." *ComputatComputational and Mathematical Methods in Medicine* 2012 (August): e130985. doi:10.1155/2012/130985, 10.1155/2012/130985.

Tukey, John Wilder. 1958. "Bias and Confidence in Not Quite Large Samples." *The Annals of Mathematical Statistics* 29 (2): 614–23. doi:10.1214/aoms/1177706647.

Turbes, C. C., G. T. Schneider, and R. J. Morgan. 1983. "Partial Coherence Estimates of Brain Rhythms." *Biomedical Sciences Instrumentation* 19: 97–102.

Van Meer, Maurits P. A., Kajo van der Marel, Kun Wang, Willem M. Otte, Soufian El Bouazati, Tom A. P. Roeling, Max A. Viergever, Jan Willem Berkelbach van der Sprenkel, and Rick M. Dijkhuizen. 2010. "Recovery of Sensorimotor Function after Experimental Stroke Correlates with Restoration of Resting-State Interhemispheric Functional Connectivity." *The Journal of Neuroscience: The Official Journal of the Society for Neuroscience* 30 (11): 3964–72. doi:10.1523/JNEUROSCI.5709-09.2010.

Varotto, Giulia, Patrik Fazio, Davide Rossi Sebastiano, Dunja Duran, Ludovico D'Incerti, Eugenio Parati, Davide Sattin, Matilde Leonardi, Silvana Franceschetti, and Ferruccio Panzica. 2014. "Altered Resting State Effective Connectivity in Long-Standing Vegetative State Patients: An EEG Study." *Clinical Neurophysiology* 125 (1): 63–68. doi:10.1016/j.clinph.2013.06.016.

Section III

Graph theory in Neuroscience

3.1 Introduction

In the last decade, several studies demonstrated that by combining a variety of different imaging technologies (functional MRI, EEG, MEG) with graph theoretical analysis, it is possible to characterize the topological properties of human brain networks. Among all the available graph indexes, clustering (local structure), characteristic path length (overall integration) and small-worldness, defined as ratio between them, represented some key topological metrics (Watts and Strogatz 1998) describing the organization of information flows in a network. These metrics allowed to distinguish different classes of network such as regular, small-world, and random networks. In fact, a small-world network has a shorter path length than a regular network (characterized by high clustering and long path lengths) but a greater local interconnectivity than a random network (characterized by low clustering coefficient and short path lengths). Several anatomical, functional neuroimaging and electro-physiological studies demonstrated that networks inferred from healthy individuals are characterized by an optimal small-world organization (He, Chen, and Evans 2007; O. Sporns, Tononi, and Edelman 2000). In contrast, brain pathology and changes in cerebral structures related to aging effects generally led to the estimation of connectivity patterns with characteristics more similar to ‘‘random’’ networks (Micheloyannis et al. 2009; Micheloyannis et al. 2006; C. J. Stam et al. 2007).

Network characterization of structural, functional or effective connectivity data is increasing (Bassett and Bullmore 2009; Cornelis J. Stam and Reijneveld 2007; Bullmore and Sporns 2009) and rests on several important motivations. Indeed complex network analysis promises to reliably (Deuker et al. 2009) quantify brain networks with a small number of neurobiologically meaningful and easily computable measures (Olaf Sporns

and Zwi 2004; Achard et al. 2006; He, Chen, and Evans 2007; Hagmann et al. 2008).

In this Section, at first graph theory will be introduced with some basic concepts and with a description of the main state of the art graph indices. In the second part instead, some application of graph theoretical approach to brain connectivity networks will be described. In particular, in each application, the graph indices will be extracted from the connectivity pattern in order to answer to specific questions.

3.2 Definition of a graph

A graph is an abstract representation of a network and it consists of a set *V* of vertices (or nodes) linked by means of edges (or connections) indicating the presence of some sort of interaction between the vertices (Figure 3.1).

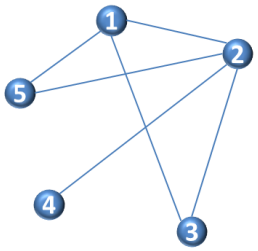

$V = \{1, 2, 3, 4, 5\}$

$E = \{\ (1,2), (1,3), (1,5), (2,3), (2,4), (2,5)\ \}$

Figure 3.1. Example of a graph with N=5 nodes and set of edges E.

A graph can be classified on the basis of two properties of the edges: weight (binary or weighted) and directionality (directed or undirected). Any weighted edge can be labelled with a weight of 0 or 1 if the existence of connections is the only aspect of interest as well as any directed graph can be symmetrized if the direction of the link is not influential in the specific application.

In neuroscience, graphs are used to represent brain connectivity with nodes modeling different brain areas and edges describing the existence of links between the activities of different anatomical regions, regardless of the

existence of an actual anatomical link. There are many estimators of brain connectivity and the use of a specific type of graph depends on the potentialities of the connectivity estimator used. Indeed with respect to the property of directionality, a graph could be:

- undirected: if the estimator is able to extract only the value of the information flows between different brain areas and not the direction;
- directed: if the estimator allows to reconstruct not only the magnitude but also the direction of the connection (e.g. Partial Directed Coherence, (Baccalá and Sameshima 2001)).

3.3 Adjacency Matrix Extraction

The mathematical representation of a graph consisting of N nodes, is the adjacency matrix A where the entry a_{ij} ($i,j=1,...,N$) is different from 0 if there is an effective link from node i to node j and equal to 0 if no link exists (Figure 3.2).

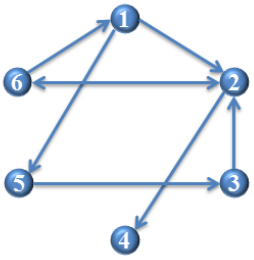

A=

0	1	0	0	1	0
0	0	0	1	0	1
0	1	0	0	0	0
0	0	0	0	0	0
0	0	1	0	0	0
1	1	0	0	0	0

Figure 3.2. Example of adjacency matrix: a 6-nodes directed graph is shown and on the right the corresponding 6x6 binary adjacency matrix is reported.

For the extraction of adjacency matrix from a connectivity network, different approaches have been developed mainly based on the following methods based on:

- threshold criteria;

- qualitative assumptions aiming at fixing or at maximizing some properties of the investigated networks.

In the first case, an edge connecting two nodes exists if the connectivity value between those nodes is above a certain threshold; otherwise the edge is null. In particular:

$$a_{ij} = \begin{cases} w_{ij} & if \;\; w_{ij} > \tau_{ij} \\ 0 & otherwise \end{cases} \tag{3.1}$$

where w_{ij} represent the value of connection from node i to node j and τ_{ij} is the corresponding threshold.

Different methodologies are available for defining such threshold and a possible approach is to select a fixed threshold. In this respect, four criteria are typically adopted: 5% significant level as a threshold fixed for discarding connectivity values from the random case (Salvador et al. 2005; Ferrarini et al. 2009); an arbitrary value in order to discard the weak connections (van den Heuvel et al., 2009); the largest possible threshold allowing all nodes to be connected at least to another node in the network (Bassett et al. 2006); asymptotic statistic method (Takahashi, Baccalà, and Sameshima 2007). The choice of the threshold should not depend on the application and if done in an arbitrary way could affect the results. In fact, the threshold influences the number of connections considered for the subsequent graph analysis and thus affects the indices extracted from the networks (van Wijk, Stam, and Daffertshofer 2010). Recently, it was demonstrated that the use of statistical thresholds computed on null-case distribution or on baseline condition allows to prevent erroneous description of network main properties (Toppi et al. 2012).

The second method to extract the adjacency matrix is to fix or maximize a certain property of investigated network. A possible approach is to fix the edge density of the graph, that is, the number of existing edges divided by the number of possible edges (Wang et al. 2009). This approach is useful if

we are interested in comparing different conditions but can produce modifications in the topology of the studied network (van Wijk, Stam, and Daffertshofer 2010).

The adjacency matrix extraction is a crucial step of the graph theory approach; in fact the method used in the process might affect the structure and the topological properties of the investigated networks.

3.4 Graph Theory Indices

Different indexes can be defined on the basis of the adjacency matrix associated to a graph. The indexes are very useful to extract synthetic and quantitative information about salient topological properties of the investigated network. In the following, the most commonly indexes used in Neuroscience are described.

3.4.1 Network density

The simplest attribute for a graph is its density *k*, defined as the actual number of connections within the model divided by its maximal capacity (Figure 3.3). The mathematical formulation of the network density is given by the following:

$$k(A) = \frac{L}{N(N-1)} = \frac{1}{N(N-1)} \sum_{i \neq j \in V} a_{ij} \quad (3.2)$$

where

- *A* is the binary adjacency matrix and a_{ij} is the entry *ij* of *A;*
- *L* is the actual number of connections;
- *N* is the number of nodes*;*
- *V=1…N* is the set of nodes within the graph.

Density ranges from 0 to 1, the sparser is a graph, the lower is its value.

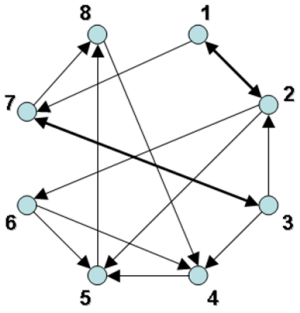

$N = 8$
$L = 15$

$$A = \begin{bmatrix} 0 & 1 & 0 & 0 & 0 & 0 & 1 & 0 \\ 1 & 0 & 0 & 0 & 1 & 1 & 0 & 0 \\ 0 & 1 & 0 & 1 & 0 & 0 & 1 & 0 \\ 0 & 0 & 0 & 0 & 1 & 0 & 0 & 0 \\ 0 & 0 & 0 & 0 & 0 & 0 & 0 & 1 \\ 0 & 0 & 0 & 1 & 1 & 0 & 0 & 0 \\ 0 & 0 & 1 & 0 & 0 & 0 & 0 & 1 \\ 0 & 0 & 0 & 1 & 0 & 0 & 0 & 0 \end{bmatrix}$$

$$k(A) = \frac{15}{56} = 0{,}268$$

Figure 3.3. Example of connection density computation. At the left of the figure, the graph consists of N=8 nodes and L=15 edges. At the right of the figure, the respective adjacency matrix is shown.

Average connection densities can vary widely, depending on the particular neural structure, on the level of analysis (i.e. populations or single cells), and on the spatial extent of the neural network (e.g. entire brain versus local circuit).

When dealing with weighted networks, a useful generalization of this quantity is represented by the weighted-density k_w. This measure evaluates the intensity of each link w_{ij} rather than the simple absence/presence of connections i.e. 0/1.

$$k_w(A) = \frac{1}{N(N-1)} \sum_{i \neq j \epsilon V} w_{ij} \tag{3.3}$$

3.4.2 Node degree

In the same way, the simplest attribute of a node is its connectivity degree, which is the total number of connections with other vertices:

$$d(i) = \sum_{j \epsilon V, i \neq j} a_{ij} \tag{3.4}$$

where V is the set of nodes and a_{ij} indicates the presence of the arc between nodes *i and j*. In the case of directed graph, this quantity has to be split into in-degree d_{in} and out-degree d_{out} (Figure 3.4). The formulation of the in-degree index d_{in} can be introduced as follows:

$$d_{in}(i) = \sum_{j \in V, j \neq i} a_{ji} \tag{3.5}$$

It represents the total amount of links incoming to the vertex *i*. *V* is the set of the available nodes and a_{ij} indicates the presence of the arc from the point *i* to the point *j*. In a similar way, for the out-degree:

$$d_{out}(i) = \sum_{j=V, j \neq i} a_{ij} \tag{3.6}$$

It represents the total amount of links outgoing from the vertex *i*. Finally the total degree of node *i* can be defined as follows:

$$d(i) = d_{in}(i) + d_{out}(i) \tag{3.7}$$

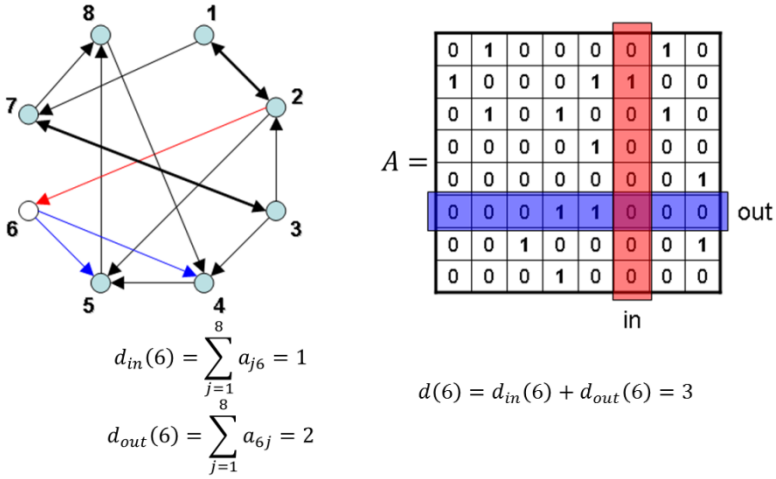

Figure 3.4. Example of in-degree and out-degree computation. At the left, the edges outgoing from the node 6 are colored in blue, while those incoming in the same node are colored in red. The rows and columns involved in the computation are colored in the adjacency matrix A.

Indegrees and outdegrees have obvious functional interpretations. A high indegree indicates that a neural unit is influenced by a large number of other units, while a high outdegree indicates a large number of potential functional targets. For most neural structures, indegrees and outdegrees of neural units are subject to constraints due to growth, tissue volume or metabolic limitations. Connections cannot be attached or emitted beyond the limits imposed by these constraints (Sporns 2002).

In a weighted graph, the natural generalization of the degree of a node *i* is the node *strength* or node weight or weighted-degree. The strength index *s* represents the total intensity associated to arcs that involve the node *i*; in directed graphs two components are considered, one for the total amount of outgoing intensity from a node (*out-strength* s_{out}) and incident intensity into it (*in-strength* s_{in}):

$$s(i) = s_{in}(i) + s_{out}(i) = \sum_{j=V, j\neq i} w_{ji} + \sum_{j=V, j\neq i} w_{ij} \quad (3.8)$$

where w_{ij} is the intensity of the link from node *i* to node *j*.

3.4.3 Network structure

Two measures are frequently used to characterize the local and global structure of graphs: the characteristic Path Length *L* and the Clustering index *C* (Wattz and Strogatz, 1998). The former measures the efficiency of the passage of information among the nodes, the latter indicates the tendency of the network to form highly connected clusters of vertices.

Characteristic Path Length. The characteristic path length is the average shortest path length in the network, where the shortest path length between two nodes is the minimum *distance* to get from one node to another. It can be defined as follows:

$$L = \frac{1}{N}\sum_{i\epsilon V} L_i = \frac{1}{N}\sum_{i\epsilon V} \frac{\sum_{j\epsilon V, i\neq j} d_{ij}}{N-1} \quad (3.9)$$

where L_i is the average distance between node i and all other nodes and d_{ij} is the distance between nodes i and j. In particular, distance definition differs between binary and weighted graphs. In the first case it corresponds to the minimum number of edges that must be traversed to get from one node to another, while in a weighted graph distance is determined on the basis of a connection-length matrix, typically obtained via a mapping from weight to length (for example an inversion of connection weight). Indeed, in a weighted network, higher connections are more naturally interpreted as shorter distances.

The number of edges in shortest weighted paths may in general exceed the number of edges in shortest binary paths, because shortest weighted paths have the minimal weighted distance, but not necessarily the minimal number of edges.

Clustering Coefficient. A large number of networks show a tendency to form links between neighboring vertices, i.e. the network topology deviates from uncorrelated random organization in which triangles are sparse: this tendency is called *clustering* (Watts and Strogatz, 1998). Therefore the clustering coefficient describes the intensity of interconnections between the neighbors of a node (Watts and Strogatz 1998). It is defined as the fraction of triangles around a node as in equation 3.10 and 3.11 for directed (Fagiolo, 2007) and undirected graph respectively:

$$C = \frac{1}{N}\sum_{i\epsilon V} \frac{t_i}{(d_i^{out}+d_i^{in})(d_i^{out}+d_i^{in}-1)-2\sum_{j\epsilon V} a_{ij}a_{ji}} \tag{3.10}$$

$$C = \frac{1}{N}\sum_{i\epsilon V} \frac{2t_i}{d_i(d_i-1)} \tag{3.11}$$

where t_i represents the number of triangles involving node *i* (see table I), d_i^{in} and d_i^{out} are the in-degree and out-degree of nodes *i* respectively and a_{ij} is the entry *ij* of adjacency matrix.

TABLE I

EQUATIONS FOR THE COMPUTATION OF THE NUMBER OF TRIANGLES INVOLVING NODE I IN BINARY GRAPHS.

undirected	**directed**
$t_i = \frac{1}{2}\sum_{j,h\in V} a_{ij}a_{ih}a_{jh}$	$t_i^{\rightarrow} = \frac{1}{2}\sum_{j,h\in V} (a_{ij}+a_{ji})(a_{ih}+a_{hi})(a_{jh}+a_{hj})$

By extending to weighted network, the weighted clustering coefficient also takes into account how much weight is present in the neighborhood of the node. There are many versions of the weighted version of clustering coefficient that consider different aspects (Saramaki et al. 2007, Barrat et al. 2004, Onnela et al , Zhang and Horvath 2005).

Global- and Local- Efficiency. A more general setup has been examined in order to investigate weighted networks. In particular, (Latora and Marchiori 2001) considered weighted networks and defined the efficiency coefficient *e* of the path between two vertices as the inverse of the shortest distance between the vertices (note that in weighted graphs the shortest path is not necessarily the path with the smallest number of edges). In the case where a path does not exist, the distance is infinite and $e = 0$. The average of all the pair-wise efficiencies e_{ij} is the global-efficiency E_g of the graph. Thus, global-efficiency can be defined as:

$$E_g = \frac{1}{N(N-1)} \sum_{i,j=1,\, i \neq j}^{N} e_{ij} = \frac{1}{N(N-1)} \sum_{i,j=1,\, i \neq j}^{N} \frac{1}{d_{ij}} \tag{3.12}$$

where *N* is the number of vertices composing the graph and d_{ij} is the distance between nodes i and j (same considerations described in "*Characteristic Path Length"* about distance definition to distinguish between weighted and binary graphs).

Since the efficiency *e* also applies to disconnected graphs, the local properties of the graph can be characterized by evaluating for every vertex *i* the efficiency coefficients of S_i, which is the sub-graph composed by the neighbors of the node *i*. The local-efficiency E_l is the average of all the sub-graphs global-efficiencies:

$$E_l = \frac{1}{N} \sum_{i=1}^{N} E_g(S_i) \tag{3.13}$$

Since the node *i* does not belong to the sub-graph S_i, this measure reveals the level of fault-tolerance of the system, showing how the communication is efficient between the first neighbors of *i* when *i* is removed.

The cluster index for a network expresses the extent to which the units within the network share common neighbours that "talk" among each other. A high cluster index *C* points to a global organizational pattern consisting of

groups of units that mutually share structural connections. However, the cluster index does not provide information about the number or size of these groups and only captures local connectivity patterns involving the direct neighbours of the central vertex (Sporns, 2002).

Global- (E_g) and local-efficiency (E_l) were demonstrated to reflect the same properties of the inverse of the average shortest path *1/PL* and the clustering index *C*. In addition, the efficiencies definition is attractive since it takes into account the full information contained in the weighted links of the graph and provides an elegant solution to handle disconnected vertices.

Clustering and characteristic path length, as well as global- and local-efficiency are key topological measures and they are widely used in literature. Another network structure measure based on described indexes is the small-worldness.

Small-worldness. A network *G* is defined as small-world network if $L_G \sim L_{rand}$ and $C_G >> C_{rand}$ where L_G and C_G represent the characteristic path length and the clustering coefficient of a generic graph and PL_{rand} and C_{rand} represent the correspondent quantities for a random graph (Watts and Strogatz, 1998). On the basis of this definition, a measure of small-worldness of a network can be introduced as follows:

$$S = \frac{C_G / C_{rand}}{L_G / L_{rand}} \tag{3.14}$$

So a network is said to be a small world network if S > 1 (Humphries and Gurney, 2008).

Network structure metrics allow to distinguish different classes of network such as regular, small-world, and random networks. In fact, a small-world network has a shorter path length than a regular network (characterized by high clustering and long path lengths) but a greater local interconnectivity than a random network (characterized by low clustering coefficient and short path lengths).

3.4.4 Motifs

By motif it is usually meant a small connected graph of *M* vertices and a set of edges forming a subgraph of a larger network with *N*>*M* nodes (Milo et al, 2002). For each *N*, there are a limited number of distinct motifs. For *N* = 3, 4, and 5, the corresponding numbers of directed motifs is 13, 199, and 9364. In the present thesis, we focus on directed motifs with N=3. The 13 different 3-node directed motifs are shown in Figure 3.7.

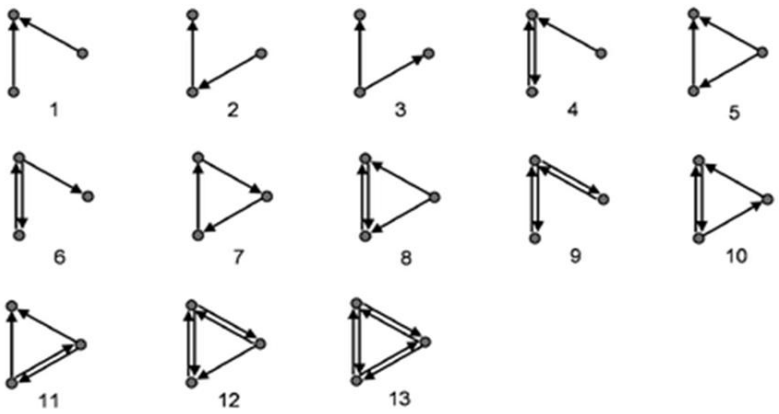

Figure 3.7. The thirteen possible motifs types that can be achieved with a sub-graph of 3 nodes.

Counting how many times a motif appears in a given network yields a frequency spectrum that contains important information on the network basic building blocks (Figure 3.8). Eventually, one can looks at those motifs within the considered network that occur at a frequency significantly higher than in random graphs.

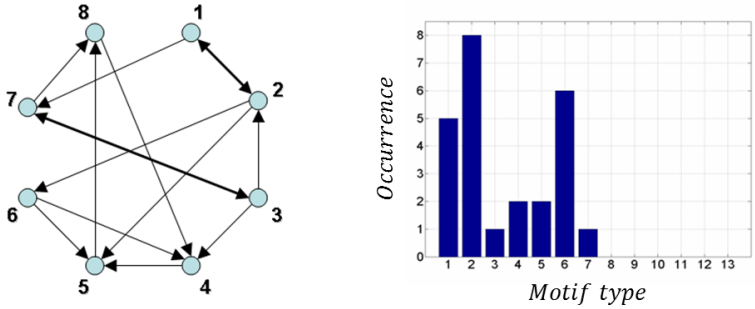

Figure 3.8. Example of 3-motif spectrum computation. At the right of the figure the 3-motif histogram associated to the graph on the left is shown: the thirteen possible motif types are displayed on the x-axes, while the occurrence of each motif is displayed on y-axes The 13 possible schemes of connectivity that can be achieved with a sub-graph of 3 nodes.

The motif frequency spectrum provides a sophisticated way of characterizing subtypes of such networks geared at more specific functional modes of information processing.

An innovative study showed that the functional motif number of a variety of real brain networks is very high compared to equivalent random networks. Motifs number can yield networks that resemble real brain networks in several structural characteristics, including their motif frequency spectra, motifs that occur in significantly increased numbers, and small-world measures (Sporns and Kotter, 2004).

3.5 Application of graph theory to effective connectivity pattern

In the previous section some applications of methods for the effective connectivity estimation and validation were described. Using different approaches, resting condition and motor task (attempted movement of the affected hand) networks were obtained starting from EEG data collected from stroke patients.

Partial Directed Coherence estimator provides directed and weighted networks: thus both binary and weighted measures can be extracted depending on the aspect under investigation. Binary indices are suitable when the focus is on the structure of the communication, while weighted measures can inform about the "power" of communication in a network.

In the following of this section, another level of investigation performed on the estimated networks will be described showing how the application of graph theory can provide measures that are able to:

- summarize brain networks properties;
- detect specific changes induced by an intervention in the communication between brain regions.

3.5.1 Network structure measures

3.5.1.1 Experimental design and Signal Analysis

The procedure developed in this thesis for the statistical assessment of changes in brain connectivity at the single subject level was tested on EEG data acquired from 12 subacute stroke patients during the execution of a motor task (attempted movement of the affected hand) as described in the previous section (*Section II - Application to real EEG data: motor task*).

Once the pattern significantly reinforced for each patient at the end of the training (POST) with respect to the PRE condition was obtained, some graph indices able to evaluate the network organization were computed to summarize the properties of these networks:

- *Characteristic Path Length;*
- *Clustering Coefficient.*
- *Global Efficiency*
- *Local Efficiency*
- *Small-Worldness.*

For each patient and frequency band, the above described measures extracted from the reinforced network (except the Smallworldness, as it is already defined taking into account random organization), were normalized with the mean value of the same indices extracted from 50 random graphs obtained maintaining the same density of its respective real data-derived graph: in this way each index (Path Length, Clustering, Global Efficiency and Local Efficiency) is independent from the network density and specifically related to the organization of the reinforced pattern

A correlation test (Pearson's correlation, significance level 0.05) was performed between the above defined neurophysiological indices based on the properties of the reinforced networks and the functional scale (FMA).

For the clinical measure, to account for the high inter-subject variability in terms of degree of the impairment, and for the consequent different level of recovery, we computed the parameter "effectiveness", which is defined as follows:

$$Eff_{FMA} = \frac{FMA_{POST} - FMA_{PRE}}{Score_{\max} - FMA_{PRE}} * 100 \qquad (3.15)$$

where $Score_{max}$ is the maximum score that can be reached in FMA scale. The effectiveness is adopted since it reflects the percentage of improvement achieved after the intervention with respect to the maximum potential improvement. Thus, if a patient achieves the highest possible score after the intervention, the effectiveness is 100%, regardless the initial score (Shah, Vanclay, and Cooper 1990). This approach allows normalization of data across patients, accounting for baseline differences. As said, the analyses were focused on connectivity patterns that were significantly reinforced for each patient in the POST with respect to the PRE session (POST vs PRE). The PRE vs POST reinforcement (inverse condition) was also tested in the

correlation analysis to check for casual effects and returned no significant results.

3.5.1.2 Results

All the obtained results of correlation analysis between graph measures of integration and segregation and the clinical outcome are reported in Table II.

TABLE II

RESULTS OF THE PEARSON CORRELATION COMPUTED BETWEEN GRAPH THEORY INDICES EXTRACTED FROM THE REINFORCED PATTERN OF MOTOR TASK AND THE CLINICAL RECOVERY MEASURED IN TERMS OF FUGL-MEYER ASSESSMENT, SIGNIFICANCES ARE HIGHLIGHTED IN BOLD.

	THETA	ALPHA	BETA1	BETA2	GAMMA
	Smallworldness				
p	0,607	0,519	**0,001**	0,597	0,123
R	0,166	0,207	**0,822**	0,170	0,471
	Path Length				
p	0,468	0,653	**0,007**	0,764	0,151
R	-0,232	-0,145	**-0,735**	-0,097	-0,441
	Clustering				
p	0,390	0,368	**0,013**	0,350	0,093
R	0,274	0,286	**0,691**	0,296	0,507
	Global Efficiency				
p	0,641	0,783	**0,004**	0,726	0,189
R	0,150	0,089	**0,765**	0,113	0,407
	Local Efficiency				
p	0,412	0,389	0,078	0,502	0,141
R	0,261	0,274	0,528	0,215	0,451

Such results show that the properties of the functional network reinforced after the training are significantly correlated with the clinical outcome. Moreover, such results are specific for the frequency band related to motor function, which was trained during the intervention (beta1, see Table II). The direct correlation between these neurophysiological measures and the clinical indices informs that the patients with higher clinical recovery show a better organization of the reinforced network related to the motor function (lower path length and higher clustering, Fig.3.9).

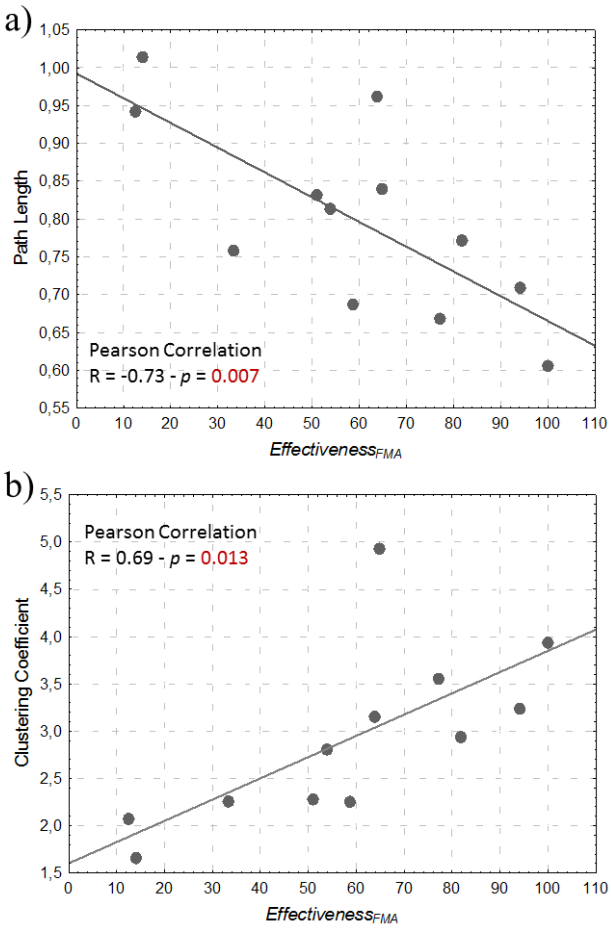

Figure 3.9. Scatter plots obtained between graph theory indices extracted from the reinforced pattern of motor task (Path Length in panel a and Clustering Coefficient in panel b) and the clinical recovery measured in terms of Fugl-Meyer Assessment in beta1 band.

3.5.2 Ad hoc measures defined for the pathology

The indexes described above do not allow to characterize the network in terms of specific properties that may be related to a specific pathology or to an intervention. This is the case of the following application for which to answer to specific questions, two new measures were defined.

3.5.2.1 Experimental design and Signal Analysis

The resting state connectivity networks, expressed as PDC matrices, were obtained for BCI and CTRL stroke patients both before and after the rehabilitative trainings (PRE and POST conditions) as described in "*Section II - Application to real EEG data: resting state*". Once the adjacency matrices were extracted by means of a statistical threshold criteria (asymptotic statistic method (Takahashi, Baccalà, and Sameshima 2007)), a graph theoretical approach was applied to provide synthetic measures that described the inter and intra-hemispheric connectivity.

3.5.2.2 Inter-hemispheric connectivity study and results

Previous studies in literature suggest that stroke may induce a reduced communication between the hemispheres (Van Meer et al, 2010; Grefkes and Fink, 2011). For this reason to describe and quantify this networks property known to be related to stroke effects, the Inter-Hemispheric Connectivity (IHC) index was defined as follows:

$$IHC = \frac{L_H}{L_{Tot}} \tag{3.16}$$

where L_H is the actual number of links connecting the two hemispheres and L_{Tot} is the actual number of connections in the whole network; in a network characterized by a given density, this index measures the portion of connections deputed to the communication between the hemispheres.

This index was used to evaluate and quantify the effects of the rehabilitative interventions in terms of rapprochement to the healthy condition. For this purpose, a group of healthy subjects (> 40 years old) was selected to build a database of normative parameters to be used for a statistical comparison with pathological subjects of comparable age.

One-way ANOVA was performed between the three groups (Healthy subjects, BCI and CTRL patients) with the Inter-Hemispheric Connections index as a dependent variable both in PRE and POST conditions.

The tests returned that both patients groups (BCI and CTRL) differ significantly from healthy population in the PRE condition (Fig. 3.10-a), whereas in POST condition the BCI group didn't show any statistically significant difference with respect to healthy population. On the contrary, such difference was still significant for the patients that had undergone a MI training without the aid of BCI (Fig. 3.10-b). These results where obtained in beta bands (beta1 and beta2).

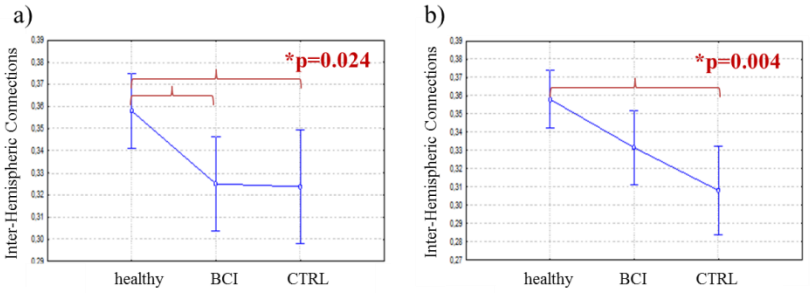

Figure 3.10. One-way ANOVA performed both in PRE and POST conditions (panel a and b respectively) between the three groups with the density of inter-hemispheric connections as a dependent variable; these results are related to beta1 band.

3.5.2.3 Intra-hemispheric connectivity study and results

The *weight* index is defined as the average value of network connections and is obtained by totaling the values of all significant PDC values divided by the number of all significant connections *L*.

This index was used to describe possible training-related changes in the estimated networks at the intra-hemispheric level; hence, *weight* was computed separately for the affected and unaffected hemispheres:

$$weight_{Hem} = \frac{\sum_{j,i \in N} w_{ji}}{L_{Hem}} \tag{3.17}$$

where w_{ij} is the value of the link between nodes i and j and L_{hem} is the number of significant connections within the hemisphere under investigation. Here, we examined whether the possible changes in the

intrahemispheric networks correlated with the behavioral outcome measure, the FMA. Specifically, the hypothesis is that a change toward a functional improvement, expressed as FMA scale effectiveness would be (positively) associated with a change toward an increase in the intra-hemispheric weight of the affected (trained) hemisphere in the BCI with respect to MI alone.

To establish consistency between the correlated measures, the variation in intra-hemispheric weight was expressed as the percentage of changes between the POST and PRE condition in the BCI and CTRL groups:

$$\Delta weight_{Hem} = \frac{weight_{Hem}^{POST} - weight_{Hem}^{PRE}}{weight_{Hem}^{PRE}} * 100 \qquad (3.18)$$

where the superscripts POST and PRE denote the 2 conditions (before and after the intervention). The new index in equation (3.18), considered to be analogous to FMA effectiveness, was calculated for each patient for both hemispheres and across frequency bands. A descriptive statistic, Pearson's correlation ($p < 0.05$), was then applied to determine the existence of a significant positive correlation (one-tailed test) between $\Delta weight_{Hem}$ and FMA effectiveness (eq. 3.16) for the experimental (BCI) and control (MI alone) interventions.

This analysis focused on intra-hemispheric connectivity measured as the Weighted Density index that allows to detect a significant positive correlation between $\Delta weight_{AH}$ (ie, the post-training percentage increase in the index value, computed for the affected hemisphere [AH]) and the effectiveness of the FMA scale in the BCI group in the beta1 (Pearson's correlation coefficient $R = 0.568$, $p = 0.034$; see Fig 3.11), beta2 ($R = 0.604$, $p = 0.024$), and gamma ($R = 0.609$, $p = 0.023$) ranges of frequency. The same index, computed for the unaffected (UH) hemisphere ($\Delta weight_{UH}$), was not significantly linked in any of the EEG frequency bands. No significant associations ($\Delta weight_{AH}$ and $\Delta weight_{UH}$) were observed in the CTRL group.

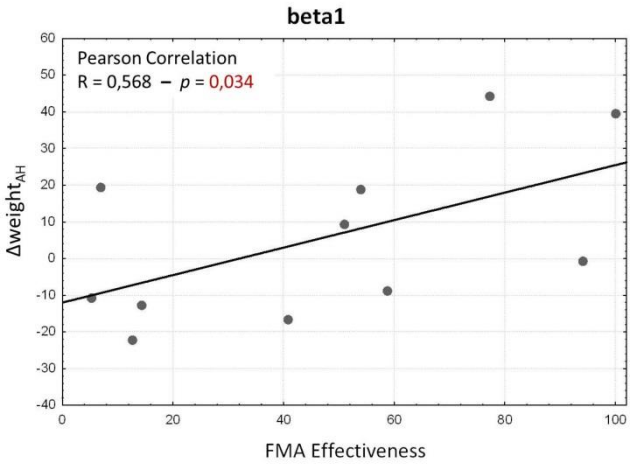

Figure 3.11. Scatter plots obtained between $\Delta weight_{AH}$ and the clinical recovery measured in terms of Fugl-Meyer Assessment in beta1 band..

3.5.3 Network Motifs Analysis

One of the main advantages in the use of the Partial Directed Coherence for the brain connectivity estimation is that it returns also the information about the direction of the causal links existing between signals. The architecture of the brain directed networks is still poorly investigated and usually the simplest and more common measures are still used to describe the communication inside a network. For example, an important measure of the network segregation is the clustering coefficient, that, as said before, measures the density of connections among a node's topological neighbors, but regardless the way in which these neighbors nodes are connected. Thus in this last section, the attention is focused to the development of advanced approaches for the interpretation of brain connectivity patterns. For instance, advanced information about the network architecture can be returned by the analysis of network motifs, constituting subgraphs or "building blocks" of the network as a whole. To apply this approach to better understand the brain organization after stroke, a network motifs analysis was performed on

resting state patterns of 45 subacute stroke patients, chronic patients (time from the event > 6 months) were excluded from the study.

3.5.3.1 Methods

PDC patterns were estimated for all the subacute stroke patients that underwent the initial screening session (N=45; mean age: 59.6 ± 13.4 years; time since event: 2 ± 1.3 months; 24 left/21 right affected hemisphere). In according to the analysis described in "*Section II - Application to real EEG data: resting state*", PDC values were calculated from 51 of 61 EEG channels (omitting the most peripheral electrode leads: Fpz, AF7, AF8, FT7, FT8, TP7, TP8, PO7, PO8, and Oz) for each frequency band (theta, alpha, beta1, beta2, gamma; defined in Section I). The validation of obtained patterns was performed by means of asymptotic statistic method (Takahashi, Baccalà, and Sameshima 2007).

As the aim of the study is to understand the architecture of resting state network after stroke, the PDC patterns were binarized and a network motifs analysis was performed considering motifs composed by 3 nodes: the possible configurations are 13, starting from the simplest to get to the more complex communication structures (see Fig. 3.7).

For each subject, the network was decomposed into a set of motifs. Once the motifs were detected, three kind of frequency with which they appear in the network can be considered:

- motifs frequencies averaged over all nodes (frequencies vector, one value for each motif type): it informs about the frequency with which a specific motif configuration appears in the network;
- motifs frequencies related to each node (2D frequency matrix, one value for each motif type and node): it informs about the occurrences with which a specific motif configuration appears in the network involving a specific node;

- motifs frequencies for each pair of nodes (3D frequency matrix: in particular one 2D matrix for each motif containing one frequency value for each couple of nodes): it informs about the occurrences with which a specific motif configuration appears in the network characterizing the communication between two nodes.

Regarding the last kind of frequency, I implemented a Matlab function to obtain this third information. An example of motifs frequencies study is shown in Figure 3.12.

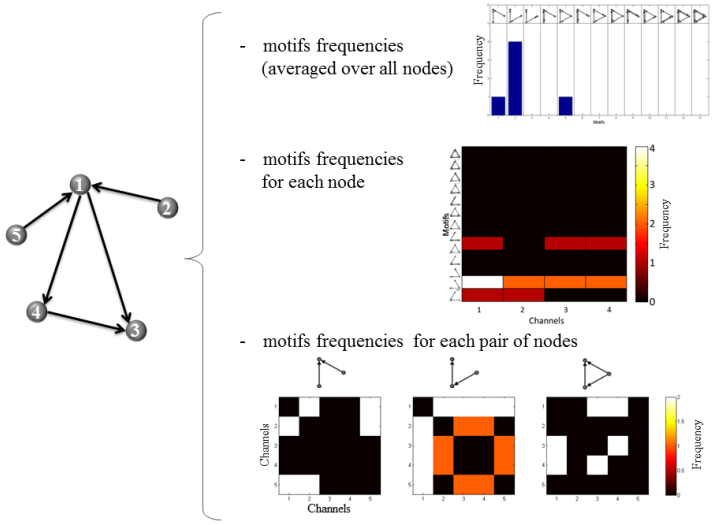

Figure 3.12. Motifs frequencies study obtained for the graph on the left.

Validation of motifs frequencies study

To validate the motifs frequencies obtained, a distribution of the null case was built by means of random graphs. The random graphs distribution was generated for each real network preserving in/out degree distribution. Only the motifs that occur at a frequency significantly different than in random graphs were considered (Milo et al, 2002). The used validation procedure for the motifs analysis is shown in Figure 3.13: Z score

normalization was used to distinguish between the motifs frequencies significantly lower and greater than in the random networks.

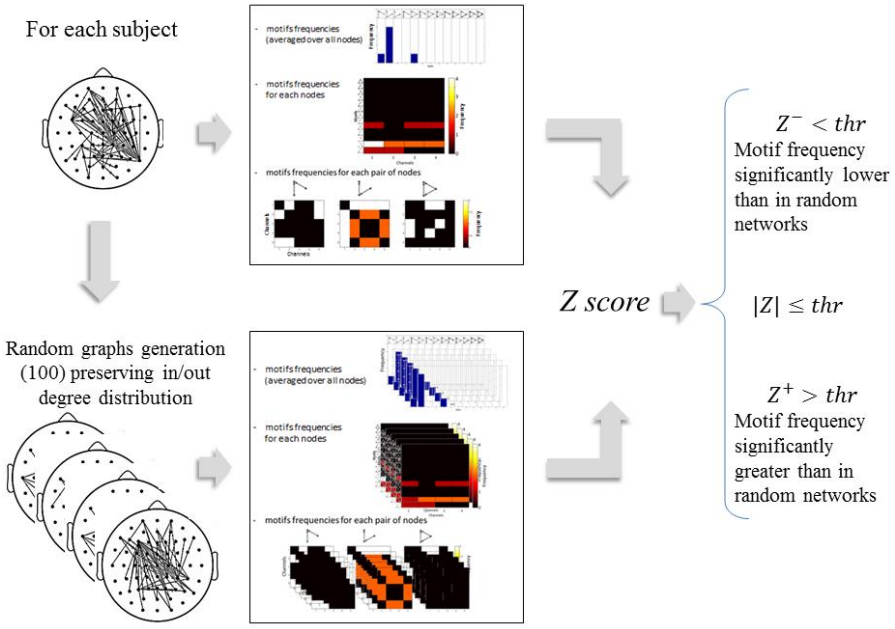

Figure 3.13. Validation procedure for the motifs analysis.

The information returned by this validation step were used to investigate the motifs configurations that characterized consistently the resting state networks of the subacute stroke population. Once the configurations were identified, the study focused only on these motifs.

Definition of new index based on network motifs analysis

As said before the third level of investigation in network motifs analysis returned a matrix (*M*) for each motif configuration (Fig 3.14a): this matrix is symmetric and the entry m_{ij} informs about the number of motifs of the specific configuration under investigation, in which the link between nodes *i* and *j* is involved.

This matrix can be organized to obtain 3 sub-blocks of interest: Affected Hemisphere (AH), Inter-Hemispheric (IH) and Unaffected Hemisphere (UH)

motifs sub-matrices. In Figure 3.14, this matrix is shown highlighting the three sub-blocks of interest. A binary version of this *M* matrix can be obtained (Fig. 3.14b). This version returns the network structure composed by 3-nodes motifs validated at the single subject level with the random graphs distribution.

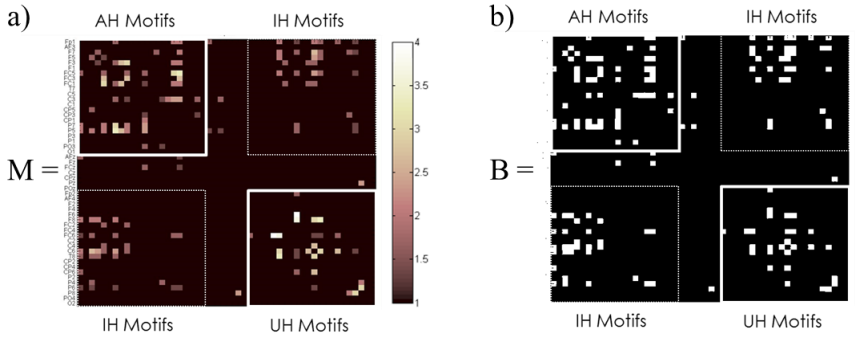

Figure 3.14. Motifs frequency matrix related to 6th configuration obtained for a stroke patient:a) weighted matrix *M*; b) binary matrix *B*. Nodes were organized to obtain 3 sub-blocks of interest: Affected Hemisphere (AH), Inter-Hemispheric (IH) and Unaffected Hemisphere (UH) sub-matrices. Color bar in panel *a* codes for the motifs frequency value.

On the basis of this rearranged binary matrix *B* (Fig. 3.14b), I defined the following new indices:

$$AH\_Motifs = \frac{\sum_{i=1}^{chAH}\sum_{j=i+1}^{chAH} b_{ij}}{chAH*chAH/2} \quad (3.19)$$

$$UH\_Motifs = \frac{\sum_{i=1}^{chUH}\sum_{j=i+1}^{chUH} b_{ij}}{chUH*chUH/2} \quad (3.20)$$

$$IH\_Motifs = \frac{\sum_{i=1}^{chAH}\sum_{j=1}^{chUH} b_{ij}}{chAH*chUH} \quad (3.21)$$

where b_{ij} is the entry of matrix *B* related to the link between nodes *i* and *j*, *chAH* and *chUH* the number of channels belonging to the affected and unaffected hemispheres respectively. These three measures (*structural* indices) can be computed considering each motif configuration and allow to capture the "architecture" of the communication within each hemisphere and between them.

Also the weighted version of the new indices was defined considering the matrix *M*:

$$wAH\_Motifs = \frac{\sum_{i=1}^{chAH}\sum_{j=i+1}^{chAH} m_{ij}}{N_{Tot}} \quad (3.22)$$

$$wUH\_Motifs = \frac{\sum_{i=1}^{chUH}\sum_{j=i+1}^{chUH} m_{ij}}{N_{Tot}} \quad (3.23)$$

$$wIH\_Motifs = \frac{\sum_{i=1}^{chAH}\sum_{j=1}^{chUH} m_{ij}}{N_{Tot}} \quad (3.24)$$

with:

$$N_{tot} = \sum_{i=1}^{ch}\sum_{j=1}^{ch} m_{ij}$$

where m_{ij} is the entry of matrix *M* related to the link between nodes *i* and *j*, *chAH* and *chUH* the number of channels belonging to the affected and unaffected hemispheres respectively and *ch* is the number of all channels.

Statistical analysis

The new indices were used for different purposes:

- to describe specific properties in the brain general organization at rest to be correlated with the outcome of the intervention, with possible prognostic value;
- to evaluate the brain plasticity phenomena.

In the first case, a correlation study (Pearson's correlation, significance level 0.05) was performed between the new weighted indices (*AH_motifs*, *UH_motifs*, *IH_motifs*) computed before the intervention (condition PRE) and FMA effectiveness.

Instead to reach the second aim, network motifs analysis was also performed on data related to the POST condition. In particular, for each patient *AH_motifs* and *UH_motifs* structural indices were computed for each frequency band and condition focusing only on the motifs configurations characterizing the resting state network and identified with previous steps.

These measures were subjected to repeated-measures ANOVA considering two within factors:

- hemisphere (2 levels: *AH_motifs*, *UH_motifs*);
- condition (2 levels: PRE, POST training).

Both the above statistical analysis were performed regardless the specific MI training (BCI-supported or MI alone).

3.5.3.2 Results

Figure 3.15 shows that the motifs characterizing the patients' networks at rest in beta1 band are related to a more complex structure (e.g. 3 nodes completely connected with each pair communicating with bidirectional link). In fact red bars in Fig. 3.15 correspond to the percentage of subjects for which the motifs frequencies related to each specific configuration are greater than in random networks. Instead blue bars are related to the opposite behavior and so in this case high patients' percentage correspond to motif configuration more characterizing random organization. The other frequency bands showed same results.

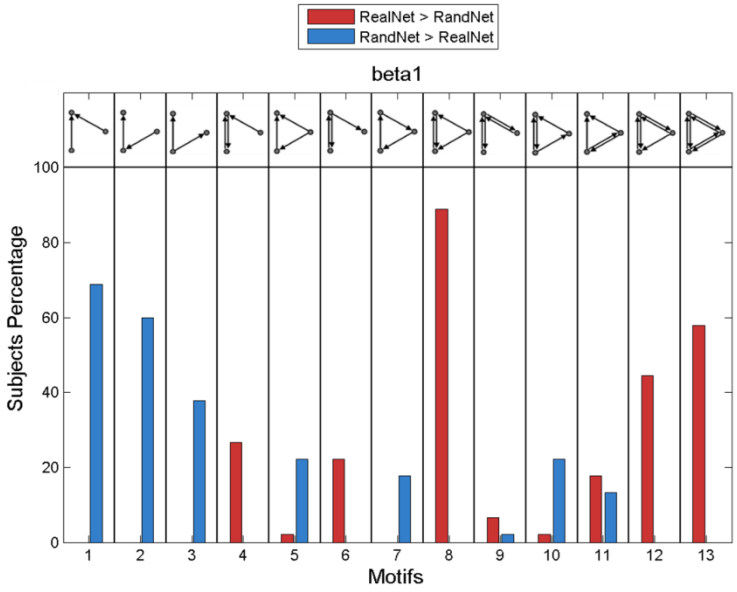

Figure 3.15. Bar diagram obtained in beta1 band. Red bars correspond to the percentage of subjects for which the motifs frequencies related to each specific configuration are greater than in random networks, while blue bars correspond to the percentage of subjects for which the motifs frequencies are lower than in random graphs.

This step of analysis allows to focus only on 4 motifs configuration (Figure 3.16)

Figure 3.16. Motifs characterizing the patients' networks at rest.

Motifs indices were computed for the selected 4 configurations and correlation analysis was performed for each index, motif and frequency band. A positive relation between IH_motifs weighted index (related to the 13th configuration) and the clinical outcome was found in theta band (Figure 3.17): higher is the Inter-hemispheric index in condition PRE, higher is the clinical recovery measured by means of FMA effectiveness.

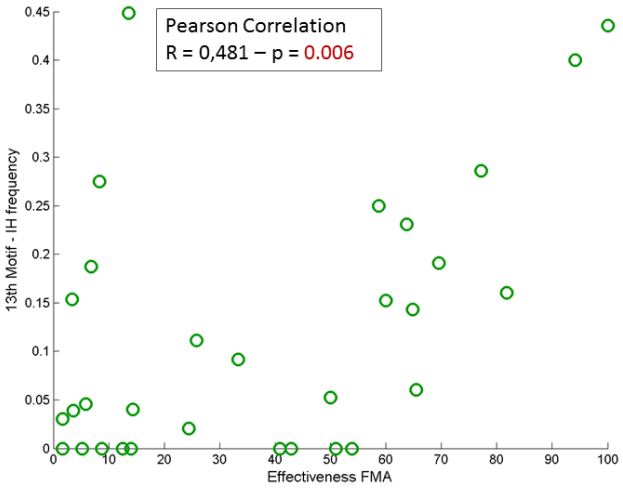

Figure 3.17. Scatter plot obtained between IH_motifs index (related to the 13th configuration) and the clinical recovery measured in terms of Fugl-Meyer Assessment in beta1 band.

At last MI training effects induced on resting state network were evaluated by means of repeated-measures ANOVA performed considering the within factors hemisphere (2 levels: AH_motifs, UH_motifs) and condition (2 levels: PRE, POST training). In figure 3.18 the results related to the 8th motif and obtained in beta1 band were shown: in PRE condition the communication in the affected hemisphere is more characterized by these complex "building blocks" with respect to the unaffected hemisphere, while in POST condition a symmetric behavior of the two hemisphere was revealed.

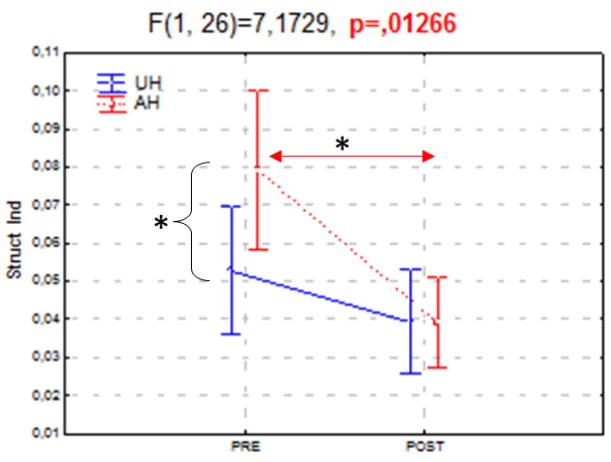

Figure 3.18. Repeated-measures ANOVA performed considering the within factors hemisphere (2 levels: AH_motifs, UH_motifs) and condition (2 levels: PRE, POST training): results related to the 8th motif and obtained in beta1 band.

3.6 Discussion and conclusion

In this section, after providing concepts at the basis of graph theory, some applications of the graph theorethical approach to brain connectivity networks were described. These applications were performed with different aims. Indeed graph indices can summarize different network properties and provide accurate descriptors of changes induced in these properties for istance as a consequence of a therapy.

3.6.1 Network structure measures

In the study of motor function pattern reinforced after the rehabilitative period, typical graph measures of segregation and integration were evaluated. These properties showed a significant correlation with the functional improvement of the affected upper limb. Such correlation between normalized indices of the network properties (normalized path length, clustering and global efficiency, and the Smallwordness, which is normalized itself) and a normalized index of the functional recovery (the effectiveness) suggests that patients with higher clinical recovery show a

better organization of the reinforced network (high clustering, low path length, high smallworldness). Consistently, such result is very specific for the frequency band that is related to motor functions, while no similar results were achieved for any other frequency bands (Table II). Interestingly, the patients in this study underwent a BCI-based intervention in add-on to their standard rehabilitation program during which they were trained to perform imagination of affected upper limb movements; such training led to a reinforcement of activation patterns in the beta1 band, as described in Section I (Pichiorri et al. 2015).

Therefore, the use of the extracted graph indices and the results obtained confirm the sensitivity of these measures in describing task-related brain networks in stroke patients. Indeed in (De Vico Fallani et al. 2013) these indices were used to characterized Motor Imagery brain network related to the imagination of movements with the affected hand with respect to the MI of the unaffected hand. Furthermore, in line with our results, Buch et al in (Buch et al. 2012) demonstrated that chronic stroke patients with more organized functional network activity (measured by means of cost efficiency index) exert better the sensorimotor rhythm modulation skill after longitudinal motor imagery training with BCI support.

Such results suggest that the combined use of procedure for the single-subject study (proposed in Section II) and graph theory approach is able to provide reliable and quantifiable neurophysiological measures of modifications in brain networks that reflect, in a significant way, the variations captured behaviorally by functional scales commonly used in the clinical practice.

3.6.2 Measures defined ad hoc for the pathology

New indices can be defined to evaluate and quantify the effects af a pathology on brain network, also useful to investigate its changes induced by

a rehabilitative intervention. These changes can be evaluated in terms of rapprochement to the healthy condition or by means of a comparison between two condition (before and after a therapy).

The procedure developed for the study of inter-hemispheric connectivity, including the building of a database of normative parameters and the use of synthetic brain indices based on specific connectivity damages, proved appropriate to quantify the effects of a rehabilitative intervention in terms of rapprochement to the healthy condition.

A new index was also defined for the study of intra-hemispheric connectivity. In this case the analysis mainly focused on the communication inside the affected hemisphere ($\Delta weight_{Hem}$, measure based on the difference between conditions PRE and POST). The hypothesis related to the obtained results is that the observed positive correlation between the increase in ipsilesional connectivity at rest in the beta and gamma oscillations and functional improvement supports the interpretation that proposed BCI training intervention effectively harness the sensorimotor rhythms in the affected hemisphere, the recruitment of which enhances the clinical improvement in the BCI group.

3.6.3 Network Motifs Analysis

The proposed network motifs analysis provides advanced information about the network architecture of resting state network after stroke. The analysis focusing on 3-nodes motifs showed that the configurations characterizing the patients' networks at rest are related to a more complex configurations (3 nodes completely connected with each pair communicating with bidirectional link), while simple configurations are typical of random organization. Furthermore the definition of new indices based on motifs analysis, allowed to investigate the architecture of hemispheres sub-networks and the inter-hemispheric communication. In particular intra-hemisphere

motifs indices revealed that after stroke in PRE condition the communication in the affected hemisphere is better characterized by these complex “building blocks” with respect to the unaffected hemisphere. The statistical analysis showed that after the rehabilitative training this asymmetry between hemisphere disappeared.

At last IH_motifs index confirmed the crucial role of inter-hemispheric connectivity after stroke: a significant correlation between this new index at rest before the intervention and the FMA effectiveness was returned in theta frequency band which is known to have an important role in the resting state networks. Such results, obtained putting in relation the brain network properties before the intervention with the subsequent clinical outcome, provide a first step toward the definition of prognostic indices based on simple EEG measures at rest.

In conclusion, all the discussed studies proved that a correct choice of graph indices to be extracted from networks under investigation, can provide accurate measures of changes in the brain organization able to:

- support a diagnosis of motor and cognitive impairments directly based on cortical modifications;
- provide a neurophysiological description of brain functional recovery;
- allow the evaluation of the effects of (conventional and innovative) rehabilitation approaches to brain re-organization;
- select a subset of indices with prognostic value, to improve, optimize and tailor the therapy for each individual patient.

Section III References

Achard, Sophie, Raymond Salvador, Brandon Whitcher, John Suckling, and Ed Bullmore. 2006. "A Resilient, Low-Frequency, Small-World Human Brain Functional Network with Highly Connected Association Cortical Hubs." *The Journal of Neuroscience: The Official Journal of the Society for Neuroscience* 26 (1): 63–72. doi:10.1523/JNEUROSCI.3874-05.2006.

Baccalá, Luiz A., and Koichi Sameshima. 2001. "Partial Directed Coherence: A New Concept in Neural Structure Determination." *Biological Cybernetics* 84 (6): 463–74. doi:10.1007/PL00007990.

Bassett, Danielle S., and Edward T. Bullmore. 2009. "Human Brain Networks in Health and Disease." *Current Opinion in Neurology* 22 (4): 340–47. doi:10.1097/WCO.0b013e32832d93dd.

Bassett, Danielle S., Andreas Meyer-Lindenberg, Sophie Achard, Thomas Duke, and Edward Bullmore. 2006. "Adaptive Reconfiguration of Fractal Small-World Human Brain Functional Networks." *Proceedings of the National Academy of Sciences of the United States of America* 103 (51): 19518–23. doi:10.1073/pnas.0606005103.

Buch, Ethan R., Amirali Modir Shanechi, Alissa D. Fourkas, Cornelia Weber, Niels Birbaumer, and Leonardo G. Cohen. 2012. "Parietofrontal Integrity Determines Neural Modulation Associated with Grasping Imagery after Stroke." *Brain: A Journal of Neurology* 135 (Pt 2): 596–614. doi:10.1093/brain/awr331.

Bullmore, Ed, and Olaf Sporns. 2009. "Complex Brain Networks: Graph Theoretical Analysis of Structural and Functional Systems." *Nature Reviews Neuroscience* 10 (3): 186–98. doi:10.1038/nrn2575.

Deuker, Lorena, Edward T. Bullmore, Marie Smith, Soren Christensen, Pradeep J. Nathan, Brigitte Rockstroh, and Danielle S. Bassett. 2009. "Reproducibility of Graph Metrics of Human Brain Functional Networks." *NeuroImage* 47 (4): 1460–68. doi:10.1016/j.neuroimage.2009.05.035.

De Vico Fallani, Fabrizio, Floriana Pichiorri, Giovanni Morone, Marco Molinari, Fabio Babiloni, Febo Cincotti, and Donatella Mattia. 2013. "Multiscale Topological Properties of Functional Brain Networks during Motor Imagery after Stroke." *NeuroImage* 83 (December): 438–49. doi:10.1016/j.neuroimage.2013.06.039.

Ferrarini, Luca, Ilya M. Veer, Evelinda Baerends, Marie-José van Tol, Remco J. Renken, Nic J. A. van der Wee, Dirk J. Veltman, et al. 2009. "Hierarchical Functional Modularity in the Resting-State Human Brain." *Human Brain Mapping* 30 (7): 2220–31. doi:10.1002/hbm.20663.

Hagmann, Patric, Leila Cammoun, Xavier Gigandet, Reto Meuli, Christopher J. Honey, Van J. Wedeen, and Olaf Sporns. 2008. "Mapping the Structural Core of Human Cerebral Cortex." *PLoS Biology* 6 (7): e159. doi:10.1371/journal.pbio.0060159.

He, Yong, Zhang J. Chen, and Alan C. Evans. 2007. "Small-World Anatomical Networks in the Human Brain Revealed by Cortical Thickness from MRI." *Cerebral Cortex (New York, N.Y.: 1991)* 17 (10): 2407–19. doi:10.1093/cercor/bhl149.

Latora, Vito, and Massimo Marchiori. 2001. "Efficient Behavior of Small-World Networks." *Physical Review Letters* 87 (19). doi:10.1103/PhysRevLett.87.198701.

Micheloyannis, Sifis, Ellie Pachou, Cornelis Jan Stam, Michael Breakspear, Panagiotis Bitsios, Michael Vourkas, Sophia Erimaki, and Michael Zervakis. 2006. "Small-World Networks and Disturbed Functional Connectivity in Schizophrenia." *Schizophrenia Research* 87 (1-3): 60–66. doi:10.1016/j.schres.2006.06.028.

Micheloyannis, Sifis, Michael Vourkas, Vassiliki Tsirka, Eleni Karakonstantaki, Kassia Kanatsouli, and Cornelis J. Stam. 2009. "The Influence of Ageing on Complex Brain Networks: A Graph Theoretical Analysis." *Human Brain Mapping* 30 (1): 200–208. doi:10.1002/hbm.20492.

Pichiorri, Floriana, Giovanni Morone, Manuela Petti, Jlenia Toppi, Iolanda Pisotta, Marco Molinari, Stefano Paolucci, et al. 2015. "Brain-Computer Interface Boosts Motor Imagery Practice during Stroke Recovery: BCI and Motor Imagery." *Annals of Neurology* 77 (5): 851–65. doi:10.1002/ana.24390.

Salvador, Raymond, John Suckling, Martin R. Coleman, John D. Pickard, David Menon, and Ed Bullmore. 2005. "Neurophysiological Architecture of Functional Magnetic Resonance Images of Human Brain." *Cerebral Cortex* 15 (9): 1332–42. doi:10.1093/cercor/bhi016.

Shah, S., F. Vanclay, and B. Cooper. 1990. "Efficiency, Effectiveness, and Duration of Stroke Rehabilitation." *Stroke; a Journal of Cerebral Circulation* 21 (2): 241–46.

Sporns, Olaf, and Jonathan D. Zwi. 2004. "The Small World of the Cerebral Cortex." *Neuroinformatics* 2 (2): 145–62. doi:10.1385/NI:2:2:145.

Sporns, O., G. Tononi, and G. M. Edelman. 2000. "Connectivity and Complexity: The Relationship between Neuroanatomy and Brain Dynamics." *Neural Networks: The Official Journal of the International Neural Network Society* 13 (8-9): 909–22.

Stam, C. J., B. F. Jones, G. Nolte, M. Breakspear, and Ph Scheltens. 2007. "Small-World Networks and Functional Connectivity in

Alzheimer's Disease." *Cerebral Cortex (New York, N.Y.: 1991)* 17 (1): 92–99. doi:10.1093/cercor/bhj127.

Stam, Cornelis J., and Jaap C. Reijneveld. 2007. "Graph Theoretical Analysis of Complex Networks in the Brain." *Nonlinear Biomedical Physics* 1 (1): 3. doi:10.1186/1753-4631-1-3.

Takahashi, Daniel Yasumasa, Luis A. Baccalà, and Koichi Sameshima. 2007. "Connectivity Inference between Neural Structures via Partial Directed Coherence." *Journal of Applied Statistics* 34 (10): 1259–73. doi:10.1080/02664760701593065.

Toppi, J., F. De Vico Fallani, G. Vecchiato, A. G. Maglione, F. Cincotti, D. Mattia, S. Salinari, F. Babiloni, and L. Astolfi. 2012. "How the Statistical Validation of Functional Connectivity Patterns Can Prevent Erroneous Definition of Small-World Properties of a Brain Connectivity Network." *ComputatComputational and Mathematical Methods in Medicine* 2012 (August): e130985. doi:10.1155/2012/130985, 10.1155/2012/130985.

Van den Heuvel, Martijn P., Cornelis J. Stam, René S. Kahn, and Hilleke E. Hulshoff Pol. 2009. "Efficiency of Functional Brain Networks and Intellectual Performance." *The Journal of Neuroscience: The Official Journal of the Society for Neuroscience* 29 (23): 7619–24. doi:10.1523/JNEUROSCI.1443-09.2009.

Van Wijk, Bernadette C. M., Cornelis J. Stam, and Andreas Daffertshofer. 2010. "Comparing Brain Networks of Different Size and Connectivity Density Using Graph Theory." *PLoS ONE* 5 (10): e13701. doi:10.1371/journal.pone.0013701.

Wang, Jinhui, Liang Wang, Yufeng Zang, Hong Yang, Hehan Tang, Qiyong Gong, Zhang Chen, Chaozhe Zhu, and Yong He. 2009. "Parcellation-Dependent Small-World Brain Functional Networks: A Resting-State fMRI Study." *Human Brain Mapping* 30 (5): 1511–23. doi:10.1002/hbm.20623.

Watts, D J, and S H Strogatz. 1998. "Collective Dynamics of 'Small-World' Networks." *Nature* 393 (6684): 440–42. doi:10.1038/30918.

Conclusion

The research activity described in this thesis was performed with the aim to address some of the methodological limitations that prevent the understanding and evaluation of changes in brain activity and connectivity related to plasticity phenomena related to rehabilitative intervention. To this purpose, different analysis methods were proposed and evaluated on electroencephalographic (EEG) signals acquired from post-stroke patients. These analyses have addressed different level of complexity in the understanding and interpretation of EEG data.

The spectral analysis was performed as first level of investigation (Section I). This approach is well known and has been ubiquitously used in the literature, as it can provide the cortical activation patterns involved in the execution of specific tasks. Even though the classic spectral analysis is still used in many different applications, in this thesis I proposed some new methodological developments with the aim to provide quantitative indices that summarize specific aspects of the brain activity, i.e.:

- the definition of a new synthetic measure of the spectral activity during motor tasks, able to quantify the entity of the desynchronization elicited in a specific scalp region;
- the definition of a new descriptor of neuroelectrical activity during BCI–assisted training that measures the trained motor-related EEG pattern.

In Section II, a second level of investigation was performed, based on the description of how the cerebral areas involved in a task are coordinated for its execution, and of how the communication between areas is modulated by a rehabilitative treatment, as a tool for studying the possible recovery of damaged brain functions (plasticity phenomena). Regarding the connectivity analysis, the main methodological contribution provided during my PhD research activity is the development of a statistical procedure for the

evaluation of changes in brain connectivity at the single subject level. After extensive simulations, the results of the application of the new statistical procedure to real data showed its feasibility in a study aimed at capturing intervention-related variations in the patients' physiological activity, i.e. in challenging conditions characterized by high individual variability.

The last section (Section III) describes an approach that can quantify the effects of pathology (or of rehabilitative interventions) in terms of synthetic measures related to the functional structure of brain networks. In particular, a new insight was provided about the use of a graph theoretical approach on brain networks, showing how the proper choice of indices to be extracted from connectivity patterns can answer specific questions raised by scientific hypothesis at the basis of a study or of a clinical problem. The applications described in this section allowed to find meaningful, stable and reliable measures that:

- provide a neurophysiological description of brain functional recovery;
- allow the evaluation of the effects of (conventional and innovative) rehabilitation approaches on the brain re-organization;
- allow selecting a subset of indices with prognostic value, to improve, optimize and tailor the therapy for each individual patient.

The results provided in this thesis showed how the application of advanced methods for the analysis of the brain activity and connectivity from EEG data can allow the extraction of meaningful, stable and reliable information in challenging conditions, like the one provided by heterogeneous, non-stationary, highly variable data gathered from post-stroke patients during a rehabilitation process.

All the methodological contributions described in this thesis were tested on data related to a specific pathology (stroke) to provide an evaluation of

their efficacy in challenging conditions and of their capability to provide answers to complex clinical questions. Anyway, they are general in their nature and can find their application in a wide range of situations provided by research and clinical applications. Their impact may thus be extended in the future to different pathological conditions, as well as to all those conditions requiring to follow the evolution of the brain reorganization in time, e.g. in learning processes, studies of the developmental age and aging.

The outcome of this thesis, resulting from the multidisciplinary integration between a methodological approach typical of the biomedical engineering and the challenges provided by clinical problems, can be seen as a possible step toward the inclusion of advanced EEG recording and analysis system in the clinical practice, as a tool to improve the diagnosis, decision and treatment of different pathological conditions.

Publications

Journal Papers

M. Petti, J. Toppi, F. Babiloni, F. Cincotti, D. Mattia and L. Astolfi: "*EEG resting state brain topological reorganization as a function of age*", *Computational Intelligence and Neuroscience* (in press)

J. Toppi and G. Borghini, **M. Petti**, E. He, V. De Giusti, B. He, L. Astolfi and F. Babiloni: *"Investigating Cooperative Behavior in Ecological Settings: An EEG Hyperscanning Study*", submitted to *PlosONE*

F. Pichiorri, G. Morone, **M. Petti**, J. Toppi, I. Pisotta, M. Molinari, S. Paolucci, M. Inghilleri, L. Astolfi, F. Cincotti, D. Mattia: *"Brain-computer interface boosts motor imagery practice during stroke recovery"*, 2015, *Annals of neurology* 77 (5), 851-865

M. Petti, J. Toppi, G. Borghini, F. Babiloni, L. Astolfi: "An EEG study on civil pilots during flight simulation", 2015, *Italian Journal of Aerospace Medicine* 1 (12)

J. Toppi, M. Risetti, L. Quitadamo, **M. Petti**, L. Bianchi, S. Salinari, F. Babiloni, F. Cincotti, D. Mattia, L. Astolfi: "*Investigating the Effects of a Non-invasive BCI Training on the Voluntary Modulation of Mental Activities: a High Resolution EEG Study"*, 2013, *Journal of Neural Engineerin*g 11 (3), 035010

4-pages Abstract to International Conferences indexed in ISI Web of Science

M. Petti, S. Caschera, A. Anzolin, J. Toppi, F. Pichiorri, F. Babiloni, F. Cincotti, D. Mattia and L. Astolfi: *Effect of inter-trials variability on the estimation of cortical connectivity by Partial Directed Coherence"*, Conf Proc IEEE Eng Med Biol Soc. 2015

M. Petti , F. Pichiorri, J. Toppi, F. Cincotti, S. Salinari, F. Babiloni, D. Mattia, L. Astolfi: *"Individual Cortical Connectivity changes after stroke: a resampling approach to enable statistical assessment at single-subject level"*, Conf Proc IEEE Eng Med Biol Soc. 2014

M. Petti, D. Mattia, F. Pichiorri, J. Toppi, S. Salinari, F. Babiloni, L. Astolf, F. Cincotti: "*A new descriptor of neuroelectrical activity during BCI–assisted Motor Imagery-based training in stroke patients"*, Conf Proc IEEE Eng Med Biol Soc. 2014

J. Toppi, A. Anzolin, **M. Petti**, F. Cincotti, D. Mattia, S. Salinari, F. Babiloni, L. Astolfi: *"Investigating Statistical Differences in Connectivity Patterns Properties at Single Subject Level: a New Resampling Approach"*, Conf Proc IEEE Eng Med Biol Soc. 2014

J. Toppi, M. Risetti, A. Anzolin, **M. Petti**, F. Cincotti, S. Salinari, F. Babiloni, D. Mattia, L. Astolfi: *"Time Varying Effective Connectivity for Describing Brain Network Changes Induced by a Memory Rehabilitation Treatment"*, Conf Proc IEEE Eng Med Biol Soc. 2014

M. Petti, J. Toppi, F. Pichiorri, F. Cincotti, S. Salinari, F. Babiloni, L. Astolfi, D. Mattia: *Aged-related Changes in Brain Activity Classification with respect to Age by means of Graph Indexes,* Conf Proc IEEE Eng Med Biol Soc. 2013

J. Toppi, **M. Petti**, G. Vecchiato, F. Cincotti, S. Salinari, D. Mattia, F. Babiloni, L. Astolfi: *The effect of normalization of Partial Directed Coherence on the statistical assessment of connectivity patterns: A simulation study,* Conf Proc IEEE Eng Med Biol Soc. 2013

J. Toppi, F. De Vico Fallani, **M. Petti**, G. Vecchiato, A. Maglione, F. Cincotti, S. Salinari, D. Mattia, F. Babiloni, L. Astolfi: *A new statistical approach for the extraction of adjacency matrix from effective connectivity networks,* Conf Proc IEEE Eng Med Biol Soc. 2013

Abstract to international conferences not indexes in ISI

D. Mattia, **M. Petti**, L. Astolfi, M. Masciullo, I. Pisotta, S. Clausi, M. Leggio, F. Cincotti, M. Molinari: *"Effects of Transcranial Direct Current Stimulation of the Cerebellum on Brain Resting State Oscillatory and Network Activity",* Conference Proceedings 45th SfN's annual meeting, Neuroscience 2015

M. Petti, D. Mattia, F. Pichiorri, L. Astolf, F. Cincotti: "*A new descriptor of neuroelectrical activity during BCI–assisted Motor Imagery training in stroke patients",* Conf Proc VI International Brain-Computer Interface Conference 2014

F. Pichiorri, **M. Petti**, J. Toppi, G. Morone, I. Pisotta, M. Molinari, L. Astolfi, F. Cincotti, D. Mattia: "Different brain network modulation following motor imagery BCI-assisted training after stroke", 30th International Conference of Clinical Neuophysiology 2014

M. Petti, F. Pichiorri, J. Toppi, F. Cincotti, S. Salinari, L. Astolfi, M. Molinari and D. Mattia: Sensorimotor oscillatory reactivity of the stroke affected hemisphere is increased by EEG-based BCI training: a study in subacute patients, IV TOBI Workshop: Practical Brain-Computer Interfaces for End-Users: Progress and Challenges, Sion, Switzerland, January 23-25, 2013 – **Oral presentation**

F. Pichiorri, G. Morone, I. Pisotta, **M. Petti**, M. Molinari, L. Astolfi, F. Cincotti, D. Mattia: BCI for stroke rehabilitation: a randomized controlled trial of efficacy, Fifth International Brain-Computer Interface Meeting: Defining the Future, June 3-7 2013 Asilomar Conference Center, Pacific Grove, California, USA

J. Toppi, L. Astolfi, M. Risetti, **M. Petti**, L.R. Quitadamo, S. Salinari, F. Cincotti, D. Mattia: Brain Mapping As a Tool To Improve a Physiologically Driven-Feature Selection for Non-Invasive BCI Applications, Fifth International Brain-Computer Interface Meeting: Defining the Future, June 3-7 2013 Asilomar Conference Center, Pacific Grove, California, USA

Abstract to national conferences

F. Pichiorri, **M. Petti**, S. Caschera, L. Astolfi, F. Cincotti, D. Mattia: *"Effective Interhemispheric Connectivity and Corticospinal Tract Integrity interdependency after unilateral stroke", XLVI Congresso della Società Italiana di Neurofisiologia 2015, Genova, Italy*

M. Petti, F. Pichiorri, G. Morone, M. Molinari, F. Cincotti, S. Salinari, F. Babiloni, D. Mattia and L. Astolfi: "Statistical assessment of cortical connectivity changes at a single-subject level: simulations and application to the evaluation of the effects of a post-stroke rehabilitative intervention", *IV Congresso del Gruppo Nazionale di Bioingegneria, Pavia 2014*

F. Pichiorri, **M. Petti**, G. Morone, M. Molinari, L. Astolfi, F. Cincotti, M. Inghilleri, D. Mattia: "Brain Network Modulation Following Motor Imagery BCI-Assisted Training After Stroke", *59° Congresso della Società Italiana Neurofisiologia Clinica 2014*

F. Pichiorri, G. Morone, **M. Petti**, I. Pisotta, M. Inghilleri, M. Molinari, S. Paolucci, L. Astolfi, F. Cincotti, D. Mattia, "Brain-Computer Interface Boosts Brain Plasticity after Stroke Leading to Improved Motor Function", *XLV Congresso della Sociatà Italiana di Neurologia 2014*

Chapters in International Books

J. Toppi, **M. Petti**, D. Mattia, F. Babiloni, L. Astolfi: "Time-Varying Effective Connectivity for Investigating the Neurophysiological Basis of Cognitive Processes", Neuromethods 2014

M. Petti and F. Babiloni: "*Graph Theory*", Neuroelectrical brain Imaging: Methods &applications, 2015

M. Petti and F. Babiloni: "*Discrete and Distributed Source Imaging*", Neuroelectrical brain Imaging: Methods &applications, 2015